

## 3. FATIGUE CRACK PROPAGATION MODELING

### 3.1 INTRODUCTION

The aim of this chapter is to present a numerical model created to analyze the fatigue behavior. The presentation of the model includes the following topics :

- representation of the crack propagation path by means of uni-dimensional elements ;
- calculation of the fatigue life of the element ;
- introduction of several important aspects of modeling ;
- explanation of the working principles of the crack closure model ;
- presentation of the working algorithm of the model.

### 3.2 REPRESENTATION OF CRACK PROPAGATION PATH

#### 3.2.1 Background

It is difficult to represent a crack tip on the basis of continuum mechanics. Such an approach, derived by Irwin [3.1] and based on Westergaard's [3.2] method to resolve the stress field at the tip of the sharp crack, results in a *singular* solution. One possibility to avoid singularity is to model the crack tip using elementary particles or blocks of a finite linear dimension  $\delta$ .

Several attempts at this have been made. Neuber [3.3] and later Harris [3.4] called this approach the microsupport concept. The microsupport concept was based on continuum mechanics. The idea of representing the structure as a sum of elemental material blocks was also analyzed by Forsyth [3.5] who wrote that “ the microstructural features in metals cause a break up of the crack front into segments that relate to elemental blocks operating with some degree of independence from their neighbors but under the general influence of the macroscopic crack of which they are a part “. Forsyth's conclusions were based on micro-scale observations of a real material. Glinka [3.6] has developed an approach where the crack growth occurs as result of the failure of elementary material blocks which were placed at the crack tip. The failure of these blocks is calculated as a function of the local strain range applied to the blocks.

It can be concluded that representation of the detail through elementary material blocks prevents the stress singularity at the vicinity of the crack tip. However, there is another argument for the use of elements: the crack initiation and the main part of the stable crack growth occurs as the result of micro-crack nucleation and growth at the stress concentrators (Section 2.3.2). This means that the fatigue crack does not grow with every load cycle but rather grows step by step. Each step of the crack growth occurs after thousands of load cycles. A step in crack growth occurs if the micro-crack(s) join the fatigue crack. The joining of the micro-crack(s) to the fatigue crack can be viewed as a failure of the element. In this regard, the use of the elements compares favorably with the physical mechanisms of the crack initiation and growth.

#### 3.2.2 Elements - Location and Numbering

It must be said that in existing approaches, only the elementary material blocks have been used to model the *crack* tip. This leads to the exclusion of the crack initiation stage from the

scope of modeling. In this study the whole *crack propagation path*<sup>1</sup> will be presented using the elementary material blocks, the *elements*<sup>2</sup>. An example of these elements located along the crack propagation path is shown in Figure 3.1.

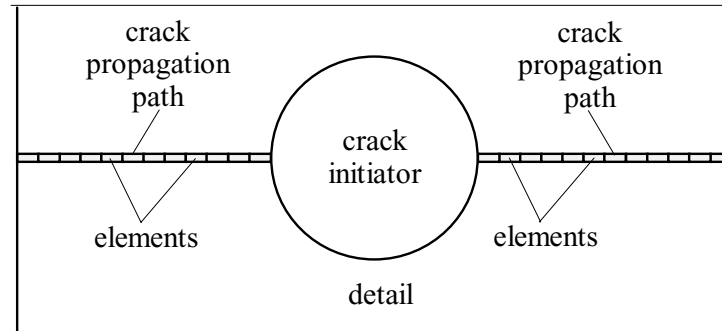


**Figure 3.1 :** Crack propagation path represented by the elements.

Two numbering systems are used to make the difference between elements : local numbering, in which numbering starts from the first non-failed element from the *stress concentrator* (Equation 3.1)

$$j = 1 \dots n_{local} \quad (3.1)$$

and global numbering, in which numbering starts from the first element from the *crack initiator* (Equation 3.2). Numbering of the elements is presented in Figure 3.2.

$$k = 1 \dots n_{global} \quad (3.2)$$

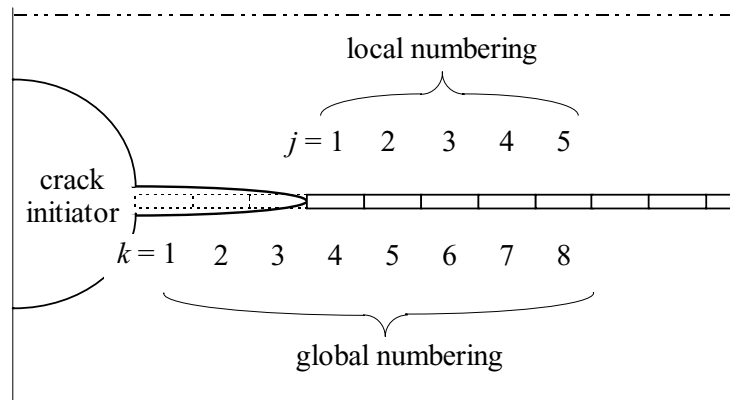


**Figure 3.2 :** Numbering of the elements.

<sup>1</sup> Analysing the linear-elastic stress field which occurs around the crack initiator, the location of the crack propagation path can be found : it is assumed that a mode I fatigue crack propagates perpendicularly to the maximum principal tensile stresses occurring in the detail.

<sup>2</sup> The elements used within this study are *not* conventional finite elements. They are a discretisation of the crack propagation path. It is assumed that each element represents the average material behaviour of a local region around it.

### 3.2.3 Element Size

In order to apply the rules of continuum mechanics to the behavior of the elements, it is very important to determine a suitable element size. The two rules which follow give the upper and lower limits for an element size. In order to satisfy the requirements of a representation within a continuous media, the element size *must* be many times greater than the size of the material grain (Equation 3.3).

$$\delta \gg \rho \quad (3.3)$$

Since local damage processes occur essentially within the plastic zone, the size of the elements *should* be smaller than the size of the smallest plastic zone possible around the stress concentrator (Equation 3.4). Both requirements for element size are presented in Figure 3.3.

$$\delta \ll r_{pl} \quad (3.4)$$

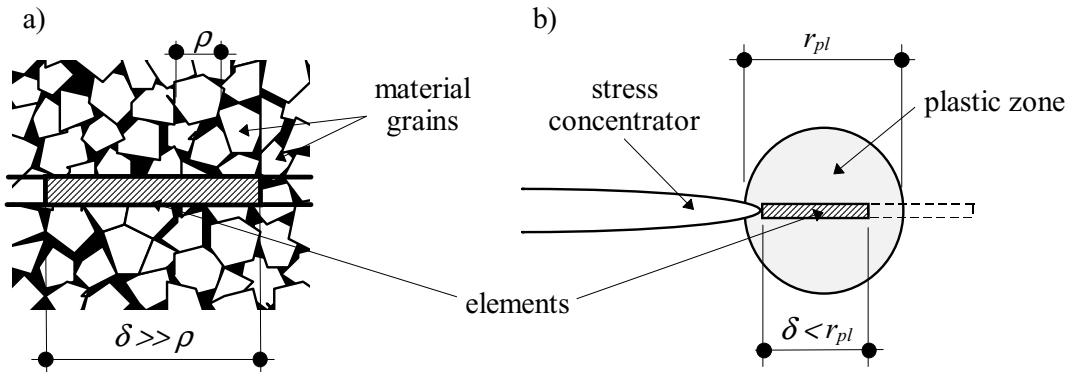


Figure 3.3 : Element size limits : a) lower limit ; b) upper limit.

The mean material grain size of most *steels* used in civil engineering is about  $\rho \approx 10^{-2}$  mm. Assuming that the requirements of continuum mechanics are satisfied if the element size exceeds 5 times the grain size, the condition (3.3) leads to the following minimum size of the element<sup>1</sup> :

$$\delta \approx 0.05 \text{ [mm]} \quad (3.5)$$

The minimum size of the plastic zone can be approximated using Equation (2.31). The stress intensity factor in Equation (2.33) can be taken :  $K_{max} \approx 250 \text{ N/mm}^{1.5}$  [3.7], [3.8]. The cyclic yield stress  $\sigma_{ys}$ , for commonly used materials does not usually exceed  $400 \text{ N/mm}^2$ . Since the plain stress state prevails after crack initiation, the plastic constraint factor can be taken :  $pcf = 1$ . Conditions (2.31) and (3.4) lead to :

$$\delta \leq \frac{\pi}{8} \left( \frac{250}{1 \cdot 400} \right)^2 = 0.153 \text{ [mm]} \quad (3.6)$$

Expressions (3.5) and (3.6) result in the conclusion that for commonly used steels, the element size should vary between the following limits :

$$0.05 \leq \delta \leq 0.15 \text{ [mm]} \quad (3.7)$$

<sup>1</sup> Since the microstructure of the aluminium differs from the microstructure of the steel, the lower limit of the elements in aluminium alloy must not correspond to the lower limit of the elements in steel.

Condition (3.7) leads to the mean value of the element size of  $\sim 0.1$  mm. This agrees with the literature data given in Annex A.2.1 about the possible element size. The influence of the element size on the modeling results is analyzed in section 5.2.1.

### 3.3 FATIGUE OF ELEMENTS

#### 3.3.1 Introduction

The representation of the crack path by the elements implies that the total fatigue life of the detail can be calculated as the sum of the fatigue lives of elements (Equation (3.8) and Figure 3.4). The aim of Section 3.3 is to illustrate the calculation of the fatigue life of element,  $N_{f,elem}$ . The physical mechanisms of the crack initiation and the stable crack growth are the same. This implies that from the beginning of the crack initiation until the end of the stable crack growth, the crack propagation should be calculated using the same principles.

$$N_f = \sum_{k=1}^{n_{global}} N_{f,elem,k} \quad (3.8)$$

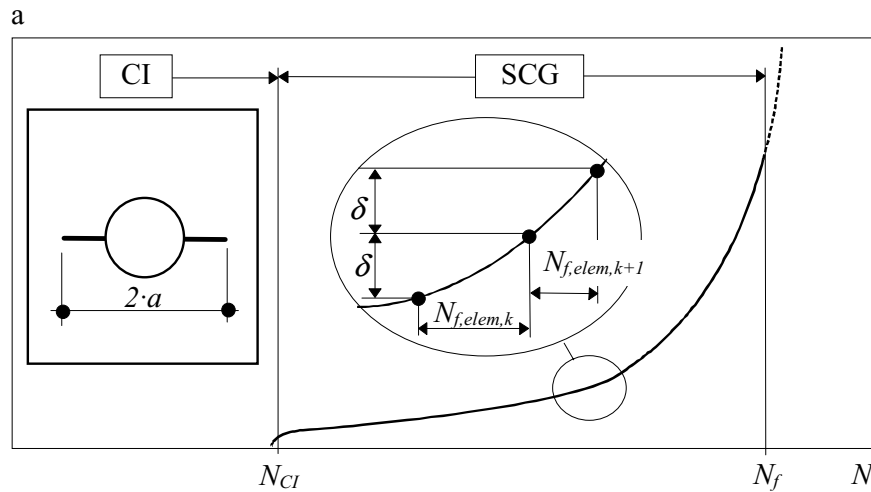


Figure 3.4 : Fatigue life as a sum of the fatigue lives of the elements.

#### 3.3.2 Load-Life Relationship

It was shown in section 2.4 that the basis of every fatigue life prediction function is a relationship between some load related parameter and fatigue life, a *load-life relationship*. In order to calculate the fatigue life of elements, an appropriate load-life relationship must be chosen.

Analyzing the three load-life relationships that were presented in Section 2.4 leads to the conclusion that the strain-life relationship (2.16) of the three relationships is the best relationship to apply to the calculation of the fatigue life of elements. The strain-life relationship is convenient because :

- the strain range,  $\Delta\varepsilon$ , needed to be introduced into the strain-life relationship, can be calculated as a function of the nominal load history and the linear elastic stress field around the stress concentrators.
- the linear elastic stress field is present around the crack initiators and the fatigue cracks and implies that the strain-life relationship can be applied to the calculation of the fatigue life

of *all* the elements, regardless if they are located at the crack initiator or at the fatigue crack.

- determination of the constants of the strain-life relationship is relatively simple as a large database of these constants exists [3.9].

The constants of the strain-life relationship are calculated by using fatigue testing on a smooth cylindrical specimen (Figure 3.5). The dimensions of the smooth specimen are different from the dimensions of the elements. However, due to the scale differences, a question arises: How can the strain-life relationship be applied to the element scale?

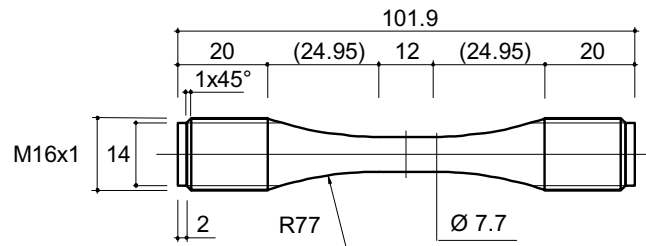


**Figure 3.5 :** A typical smooth fatigue test specimen.

The restrictions to the application of the strain-life relationship in calculating the fatigue life of the element will be discussed further. Each of the three elements presented on Figure 3.6 have one side on the surface and other sides which are surrounded by material. It is assumed that the three elements behave similarly when loaded with an equal amount of strain range  $\Delta\varepsilon$ . The fatigue life of the element at the specimen surface (case 1 in Figure 3.6) equals the *crack initiation* life of a smooth specimen. Since it was assumed that all three elements behave similarly, the total fatigue life of the elements located close to the tip of the crack or the crack initiators (cases 2 and 3 in Figure 3.6) can be calculated using the crack initiation life  $N_{CI}$  of the smooth specimen.

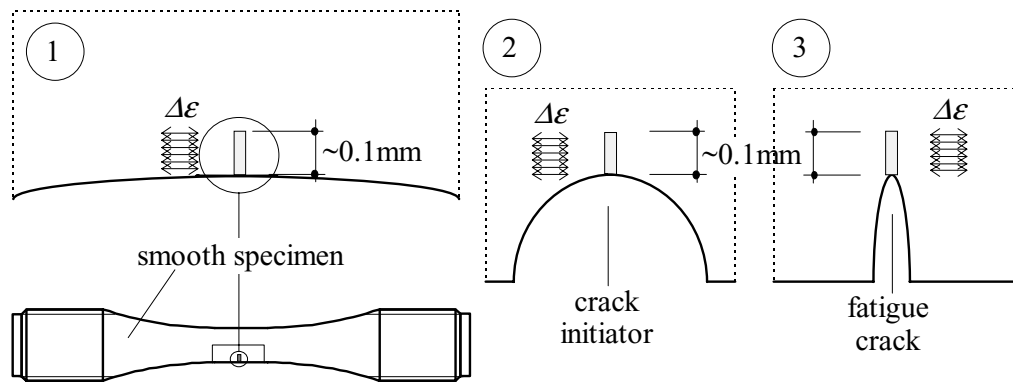


**Figure 3.6 :** Material volumes with a similar behavior.

Test results show that the ratio of the crack initiation life to the total fatigue life of a smooth specimen  $r_{CI}$  is about 80% to 90% of the total fatigue life of the smooth specimen<sup>1</sup> [3.9] :

<sup>1</sup> The crack initiation stage in a *smooth test specimen* lasts considerably longer than the stable crack growth stage. This can be explained by the almost uniform simultaneous damaging of the whole critical section. The specimen has already become very damaged by the end of the crack initiation stage due to the simultaneous

$$r_{CI} = \frac{N_{CI}}{N_f} = 0.8 \dots 0.9 \quad (3.9)$$

In order to apply the strain-life relationship (2.16) to the calculations of the fatigue life of the element, the fatigue life obtained from Equation (2.16),  $N_f$ , must be reduced by factor  $r_{CI}$ :<sup>1</sup>

$$N_{f,elem} = r_{CI} \cdot N_f \quad (3.10)$$

It is assumed that if the element and the smooth specimen are loaded by the same strain range  $\Delta\epsilon$  and if the material around the element is the same as the material of the smooth specimen, then the fatigue life of the element,  $N_{f,elem}$ , equals the crack initiation life,  $N_{CI}$ , of the smooth specimen. The strain-life relationship to apply to the elements is

$$\frac{\Delta\epsilon}{2} = \frac{\sigma'_f - \sigma_m}{E} \cdot (2 \cdot N_{f,elem})^{b'} + \epsilon'_f \cdot (2 \cdot N_{f,elem})^{c'} \quad (3.11)$$

where the  $N_{f,elem}$  in Equation (3.11) can be calculated using Equation (3.10). The determination of the constants of the strain-life relationship was explained in section 2.4.2.

The unknowns in Equation (3.11) are the strain range  $\Delta\epsilon$  and the mean stress  $\sigma_m$ . Both the  $\Delta\epsilon$  and the  $\sigma_m$  in Equation (3.11) can be determined as a function of their response on the cyclic loading. Briefly, the strain range and the mean stress of each element are a function of the loading of the element as well as the response of the element on loading. Two aspects will be reviewed in the following two sections : loading of elements and load response of elements.

### 3.3.3 Loading of the Elements

It is assumed that the elements at the stress concentrators are loaded by the *linear-elastic* cyclic stress field which occurs around the stress concentrators as result of the nominal cyclic loading. The aim of this section is to establish the relationships between the linear-elastic stress field located around the stress concentrators and the loading of the elements.

Each element represents the *average* material behavior over the length  $\delta$  and it is assumed that the distribution of the loads along an element is *uniform* (Figure 3.7). The load of element  $k$ ,  $\sigma_{le,k}$ , can be defined as an average value of the linear-elastic stress,  $\sigma_{le}(x)$ , applied onto element  $k$ . The  $\sigma_{le,k}$  can be calculated by integrating the linear-elastic stress,  $\sigma_{le}(x)$ , over the element  $k$  and dividing the result of integration by the element's size,  $\delta$ :

$$\sigma_{le,k} = \frac{1}{\delta} \int_{x_{0,k}}^{x_{0,k}+\delta} \sigma_{le}(x) dx \quad (3.12)$$

Equation (3.12) is also valid if local numbering,  $j$ , of elements is used. Due to the fact that the calculation of the linear elastic stress,  $\sigma_{le}(x)$ , in Equation (3.12) depends on the type of stress concentrator, the formulas of the loading of elements will be derived separately for the elements at the crack initiators and for the elements at the fatigue crack tip.

---

damaging of the material inside; consequently, the stable crack growth lasts for a very short time period (about 10% to 20% of total fatigue life).

<sup>1</sup> "Material Data for Cyclic Loading", [3.9], contains more than 600 sets of the strain-life relationship constants for more than a hundred different materials and alloys. Typically, the failure criterion of these tests is complete rupture of the specimen. In some cases, however, the failure criterion is the crack initiation. If the failure criterion of the smooth specimen fatigue test was crack initiation, then  $r_{CI} = 1$  in Equation (3.10).

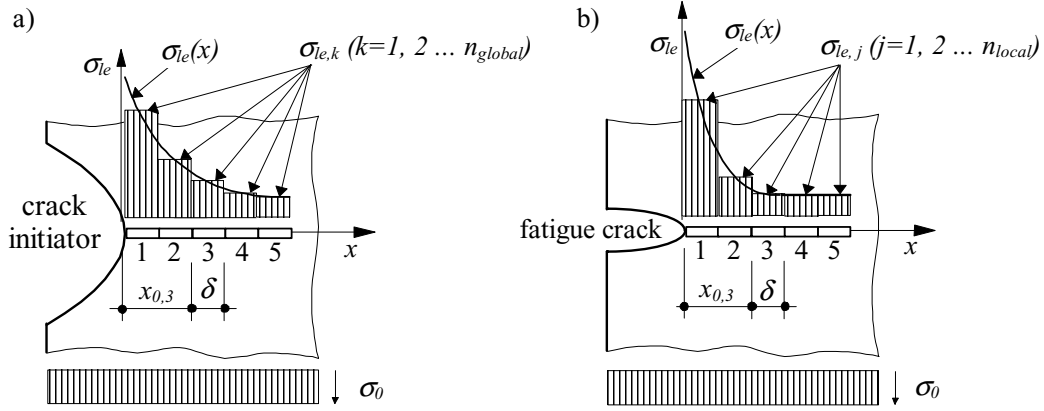


**Figure 3.7 :** Loading of the elements : a) elements at crack initiator ; b) elements at fatigue crack tip.

### Elements at the Crack Initiator

The linear-elastic stress at the *crack initiator* for any value of coordinate  $x$ ,  $\sigma_{le}(x)$ , can be calculated by using Equation (3.13) :

$$\sigma_{le}(x) = SCF(x) \cdot \sigma_0 \quad (3.13)$$

where the stress concentration factor  $SCF(x)$  in Equation (3.13) can be calculated using Equation (2.1). The edge coordinate of the element  $k$ ,  $x_{0,k}$ , in Equation (3.12) can be expressed using global numbering of the element  $k$  and the element size  $\delta$  :

$$x_{0,k} = \delta \cdot (k - 1) \quad (3.14)$$

A formula for  $\sigma_{le,k}$  can be obtained by replacing  $\sigma_{le}(x)$  in Equation (3.12) with the right side of Equation (3.13) and by replacing  $x_{0,k}$  in Equation (3.12) with the right side of Equation (3.14):

$$\sigma_{le,k} = \frac{\sigma_0}{\delta} \int_{\delta(k-1)}^{\delta k} SCF(x) dx \quad (3.15)$$

In order to account for the effect of fabrication-introduced *residual stress*, the stress concentration factor  $SCF(x)$  in Equation (3.15) must be calculated by using Equation (2.2) instead of Equation (2.1).

### Elements at the Fatigue Crack

The linear-elastic stress at the tip of *sharp fatigue crack* for any value of coordinate  $x$ ,  $\sigma_{le}(x)$ , can be calculated by using the effective stress intensity factor  $K_{eff}$  :

$$\sigma_{le}(x) = \frac{K_{eff}}{\sqrt{2 \cdot \pi \cdot x}} \quad (3.16)$$

The effective stress intensity factor  $K_{eff}$  in Equation (3.16) accounts for the crack closure effect (see Clause 2.3.3). The  $K_{eff}$  can be calculated from the stress intensity factor,  $K$ , in the aid of a crack closure model (Figure 3.8). The crack closure model is introduced in Clause 3.4.5.

In order to account for the effect of fabrication-introduced *residual stress*, the stress intensity factor  $K$  in Figure 3.8 must be calculated by using Equation (2.9) instead of Equation (2.7).

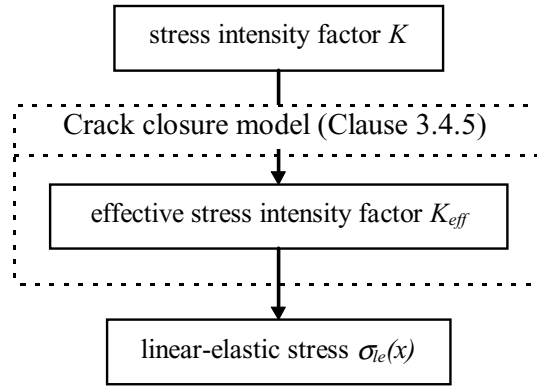


**Figure 3.8 :** Calculation algorithm of the linear-elastic stress as a function of the stress intensity factor.

The edge coordinate of the element  $j$  at the crack tip,  $x_{0,j}$ , in Equation (3.12) can be expressed by using local numeration of the element,  $j$ , and element size  $\delta$ :

$$x_{0,j} = \delta \cdot (j - 1) \quad (3.17)$$

A formula for  $\sigma_{le,j}$  can be found by replacing  $\sigma_{le}(x)$  in Equation (3.12) with the right side of Equation (3.16) and by replacing  $x_{0,k}$  in Equation (3.12) with the right side of Equation (3.17), then integrating Equation (3.12).

$$\sigma_{le,j} = K_{eff} \cdot \sqrt{\frac{2}{\pi \cdot \delta}} \cdot (\sqrt{j} - \sqrt{j-1}) \quad (3.18)$$

Equation (3.18) is valid for the *sharp* fatigue crack. In Annex A.2.2, equations which are similar to Equations (3.16) and (3.18) are given for the *blunted* fatigue crack<sup>1</sup>.

### 3.3.4 Load Response of the Elements

In the previous section, formulas that calculated the loading of the elements were given. According to these formulas, the loading of the elements located near the stress concentrators is very high (see Figure A.1). This implies that the load response of these elements is *elastic-plastic*<sup>2</sup>. The aim of this section is to derive relationships to calculate the *elastic-plastic* load response of the elements as a function of the *linear-elastic* loading of the elements.

#### *Elastic-Plastic Stress-Strain Behavior of the Elements*

Herein, the load response of elements refers to their stress-strain behavior. Before the relationships between the loading of the elements and the load response of the elements can be derived, the assumptions concerning the elastic-plastic stress-strain behavior of elements must be introduced. It is assumed that the elements behave like uni-axially loaded bodies. The cyclic elastic-plastic stress-strain curve of uni-axially loaded bodies can be given in the form of the Ramberg-Osgood equation [3.10], [3.11] :

<sup>1</sup> Annex A.2.2 also provides the comparison between the loading of the elements at the tip of the sharp and blunted cracks. The difference is less than 5%. Regardless of the fact that the tip of a real fatigue crack is always blunted, Equation (3.18) is used in the model. Chapter 5 contains the parametric study of the influence of the crack tip *bluntness* on the results of modelling.

<sup>2</sup> Load response of the elements situated *far* from the stress concentrators usually remains linear-elastic.

$$\varepsilon = \frac{\sigma}{E} + \left( \frac{\sigma}{K'} \right)^{\frac{1}{n'}} \quad (3.19)$$

It is assumed that the stress-strain *hysteresis loops* created during cyclic loading can also be described by means of Equation (3.19) in the form:

$$\frac{\Delta\varepsilon}{2} = \frac{\Delta\sigma}{2 \cdot E} + \left( \frac{\Delta\sigma}{2 \cdot K'} \right)^{\frac{1}{n'}} \quad (3.20)$$

Material constants  $K'$  and  $n'$  in Equations (3.19) and (3.20) can be found in the literature or determined by using cyclic testing [3.9], [3.10], [3.11], [3.12].

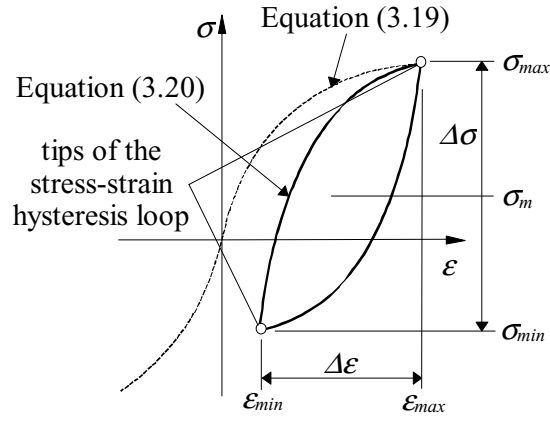


**Figure 3.9 :** Elastic-plastic stress-strain behavior of a cyclically loaded element (load response of the element).

Figure 3.9 presents the cyclic stress-strain curve (Equation 3.19) and the stress-strain hysteresis loops (Equation 3.20). It can be seen that cyclic mean stress  $\sigma_m$  depends on the position of the stress-strain hysteresis loops in the  $\sigma$ - $\varepsilon$  diagram. The position of the stress-strain hysteresis loop depends on the coordinates of its tips ( $\varepsilon_{max}$ ,  $\sigma_{max}$ ) and ( $\varepsilon_{min}$ ,  $\sigma_{min}$ ). If the coordinates of the tips of the stress-strain hysteresis loop are known, then the cyclic mean stress,  $\sigma_m$ , and the cyclic strain range,  $\Delta\varepsilon$ , of elements can be calculated using Equations (3.21) and (3.22) accordingly<sup>1</sup>.

$$\sigma_m = \sigma_{max} - \frac{\Delta\sigma}{2} \quad (3.21)$$

$$\Delta\varepsilon = \varepsilon_{max} - \varepsilon_{min} \quad (3.22)$$

The calculation of the *tips* of the stress-strain hysteresis loops is relatively complex depending on the load history applied to the body. The calculation algorithm of the tips of the stress-strain hysteresis loops as a function of any loading history is presented in Clause 3.4.1.

### **Glinka's ESED and ESED Range Criteria**

Before establishing the relationships between the linear-elastic loading of the elements and the elastic-plastic load response of the elements, Glinka's *equivalent strain energy density* criterion (ESED criterion) and equivalent strain energy density *range* criterion (ESED range

<sup>1</sup> Both  $\Delta\varepsilon$  and  $\sigma_m$  are unknowns in the strain-life relationship (3.11).

criterion) will be introduced. These criteria allow for the correlation between the stresses which are calculated on the basis of the linear-elastic stress-strain analysis, to the elastic-plastic stresses and strains occurring within the plastic zone<sup>1</sup>.

The ESED criterion was introduced by Molski and Glinka [3.13]. Glinka also extended the ESED criterion to multi-axial loading [3.14]. Hutchinson [3.15] has shown that the ESED criterion is valid when a material is characterized by a bilinear stress-strain behavior. Glinka [3.16] mentions that the strain energy density method, when corrected for plastic yielding, produces good results almost to the point of general plastic yielding of the section.

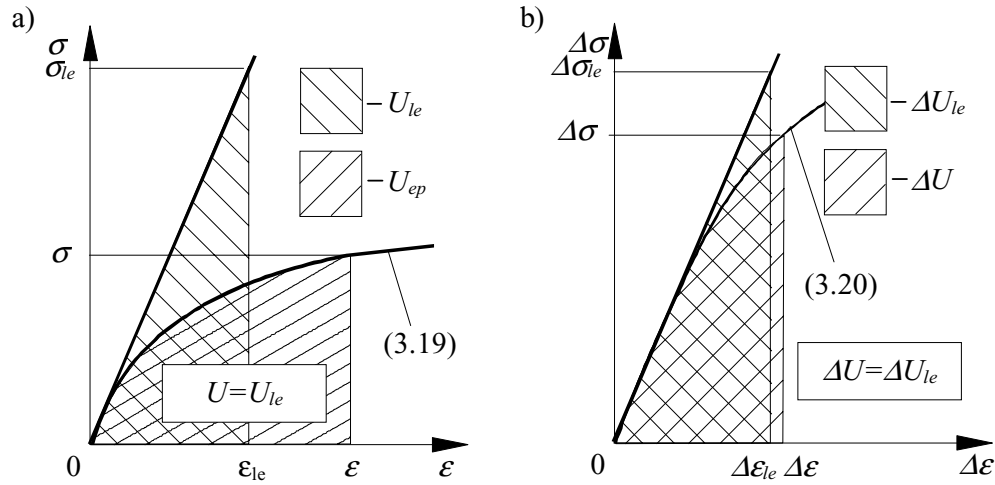


**Figure 3.10 :** Graphical presentation of Glinka's : a) ESED criterion ; b) ESED range criterion.

The ESED criterion is based on the assumption that the *elastic-plastic* strain energy density in the plastic zone is the same as the strain energy density, calculated on the basis of a *linear-elastic* stress-strain analysis (Equation 3.23). The ESED range criterion is similar to the ESED criterion : it is assumed that the elastic-plastic strain energy density *range* in the plastic zone is the same as the strain energy density *range*, calculated on the basis of a linear-elastic stress-strain analysis (Equation 3.24).

$$U = U_{le} \quad (3.23)$$

$$\Delta U = \Delta U_{le} \quad (3.24)$$

Equations (3.23) and (3.24) are graphically presented in Figure 3.10. The strain energy density and the strain energy density *range* in Figure 3.10, correspond to the area under the  $\sigma$ - $\varepsilon$  diagram and the area under the  $\Delta\sigma$ - $\Delta\varepsilon$  diagram.

### **Relationships between Loading and Load Response of the Elements**

With the ESED criterion, it is possible to relate the loading of the elements to the load response of the elements. When the loading of the elements was evaluated in terms of the

<sup>1</sup> Neuber's rule, a method similar to Glinka's ESED criterion exists. Both methods are based on similar assumptions, but Neuber's rule quantitatively overestimates the non-linear strain near the stress concentrators [3.14], [3.16]. Herein only Glinka's ESED criterion is represented. Neuber's rule is given in Annex A.2.3. In the model, Glinka's ESED criterion is used, but in Chapter 5, the influence of both methods on the modelling results is studied.

linear-elastic stresses, the load response of the elements was assumed to occur as the elastic-plastic stress-strain behavior of elements. The relationship between the loading of the elements and load response will be developed on the basis of Glinka's ESED criterion and ESED range criterion. The relationship between loading (L) and the load response (LR) of elements is abbreviated as the L-LR relationship.

The L-LR relationship between the linear-elastic stress and the elastic-plastic stress and strain will be derived based on the ESED criterion (3.23) : the linear-elastic strain energy density,  $U_{le}$ , in Equation (3.23) can be calculated by using Equation (3.25)

$$U_{le} = \frac{\sigma_{le}^2}{2 \cdot E} \quad (3.25)$$

where the  $\sigma_{le}$  is the stress calculated by using the linear-elastic approach. The elastic-plastic strain energy density,  $U$ , can be found by integrating Equation (3.19). This leads to Equation (3.26) :

$$U = \frac{\sigma^2}{2 \cdot E} + \frac{\sigma}{n'+1} \cdot \left( \frac{\sigma}{K'} \right)^{\frac{1}{n'}} \quad (3.26)$$

By replacing the right side of the ESED criterion (3.23) with the right side of Equation (3.25) and the left side of the ESED criterion (3.26) with the right side of Equation (3.26), a L-LR relationship between the linear-elastic stress,  $\sigma_{le}$ , and the elastic-plastic stress,  $\sigma$ , (Equation 3.27) results in which the  $\sigma$  can be determined by iterating Equation (3.27). The elastic-plastic strain  $\varepsilon$ , can be calculated using Equation (3.19).

$$\frac{\sigma_{le}^2}{2 \cdot E} = \frac{\sigma^2}{2 \cdot E} + \frac{\sigma}{n'+1} \cdot \left( \frac{\sigma}{K'} \right)^{\frac{1}{n'}} \quad (3.27)$$

Based on the ESED *range* criterion (3.24), the L-LR relationship between the linear-elastic stress *range* and the elastic-plastic stress and strain *ranges* can be derived : the linear-elastic strain energy density range,  $\Delta U_{le}$ , in Equation (3.24) can be calculated by using Equation (3.28) :

$$\Delta U_{le} = \frac{\Delta \sigma_{le}^2}{2 \cdot E} \quad (3.28)$$

where the  $\Delta \sigma_{le}$  is the stress range calculated by using the linear-elastic approach. The elastic-plastic strain energy density range,  $\Delta U$ , can be found by integrating Equations (3.20) which leads to Equation (3.29).

$$\Delta U = \frac{\Delta \sigma^2}{2 \cdot E} + \frac{2 \cdot \Delta \sigma}{n'+1} \cdot \left( \frac{\Delta \sigma}{2 \cdot K'} \right)^{\frac{1}{n'}} \quad (3.29)$$

By replacing the right side of the ESED range criterion (3.24) with the right side of Equation (3.28) and the left side of the ESED range criterion (3.24) with the right side of Equation (3.29), a L-LR relationship between the linear-elastic stress range,  $\Delta \sigma_{le}$ , and the elastic-plastic stress range,  $\Delta \sigma$ , (Equation 3.30) results in which the  $\Delta \sigma$  can be determined by iterating Equation (3.30). The elastic-plastic strain range  $\Delta \varepsilon$ , can be calculated using Equations (3.20).

$$\frac{\Delta \sigma_{le}^2}{2 \cdot E} = \frac{\Delta \sigma^2}{2 \cdot E} + \frac{2 \cdot \Delta \sigma}{n'+1} \cdot \left( \frac{\Delta \sigma}{2 \cdot K'} \right)^{\frac{1}{n'}} \quad (3.30)$$

### 3.3.5 Summary

At the beginning of Section 3.3 the assumption that the fatigue life of the detail is equal to the sum of the fatigue lives of the elements was made. Various aspects of the calculation for the fatigue life of the element were subsequently discussed. These aspects are now combined in a calculation algorithm. The algorithm shows the calculation procedure which can determine the fatigue life of the element<sup>1</sup> (Figure 3.11).

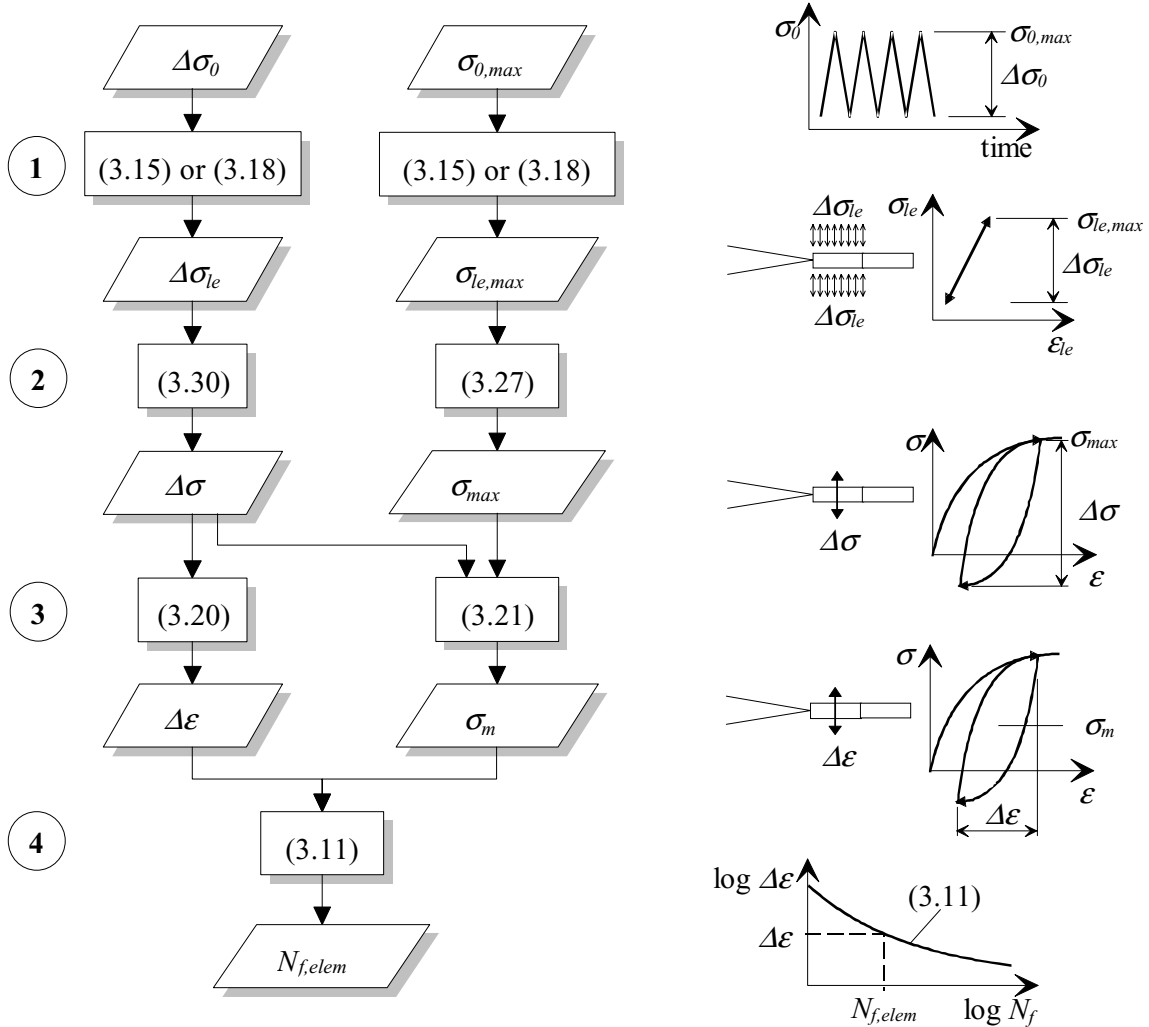


**Figure 3.11 :** Calculation algorithm of the fatigue life of the element..

The four calculation steps are :

1. Calculation of the load range,  $\Delta\sigma_{le}$ , and the maximum load,  $\sigma_{le,max}$ , applied on the element under consideration. Both  $\Delta\sigma_{le}$  and  $\sigma_{le,max}$  are determined as a function of nominal loading. For elements situated at the stress concentrator, Equation (3.15) must be used; for elements situated at the tip of the fatigue crack, Equation (3.18) must be used ;

<sup>1</sup> This algorithm can be applied only if the elements are loaded by constant-amplitude loads. The calculation of the fatigue life of the element under variable-amplitude loading is complex and is presented in Clause 3.4.2.

2. Calculation of the elastic-plastic stress range  $\Delta\sigma$  and the elastic-plastic maximum stress  $\sigma_{max}$ . This can be done by using Equations (3.30) and (3.27) accordingly. The  $\Delta\sigma$  and  $\sigma_{max}$  are calculated as a function of the linear-elastic stress range  $\Delta\sigma_{le}$ , and stress  $\sigma_{le,max}$  ;
3. Calculation of the elastic-plastic strain range  $\Delta\varepsilon$  and the elastic-plastic mean stress  $\sigma_m$ . This can be done by using Equations (3.20) and (3.21) ;
4. Calculation of the fatigue life of the element,  $N_{f,elem}$ . The fatigue life of the element is a function of the  $\Delta\varepsilon$  and  $\sigma_m$ , and it can be found by using Equation (3.11).

### 3.4 SELECTED ASPECTS OF MODELLING

In Sections 3.2 and 3.3, the *basis* of the fatigue crack propagation model was presented. There are, however, some modeling-related *aspects* which need to be addressed.

#### 3.4.1 Stress-Strain Hysteresis Loops

The elastic-plastic mean stress of the element,  $\sigma_m$  depends upon the position of the hysteresis loops on the  $\sigma$ - $\varepsilon$  diagram (Figure 3.11). The calculation algorithm presented in Figure 3.11 only considered the constant-amplitude loading. The aim of this section is to explain the calculation of the position of the stress-strain hysteresis loops of the elements for *any* nominal loading history.

The formation of the stress-strain hysteresis loops occurs according to *material memory effect*. Caligiana [3.17] stated: «...In a periodical complex history, after the cyclic ‘stabilization’ of the material, larger hysteresis loops always enclose smaller ones. If a small strain excursion occurs inside a larger strain excursion, the larger hysteresis loop is not affected by the smaller one and the hysteresis history after the closure of the smaller loop behaves as if the smaller loop had never happened. *The material ‘remembers’ the previous loading path...* ».

The position of a hysteresis loop is determined by the coordinates of its tips ( $\varepsilon_i$ ,  $\sigma_i$ ) and ( $\varepsilon_i^*$ ,  $\sigma_i^*$ ). The calculation of the elastic-plastic stress  $\sigma_i$ , and the elastic-plastic strain  $\varepsilon_i$ , at the tip  $i$  of the hysteresis loop, can be executed by using the following four steps (Figure 3.12) :

1. Calculate the elastic-plastic stress range  $\Delta\sigma_i$  and the elastic-plastic strain range  $\Delta\varepsilon_i$ , as a function of the linear elastic load  $\Delta\sigma_{le,i}$  applied to element, where  $\Delta\sigma_{le,i}$  can be found by using Equation (3.31).

$$\Delta\sigma_{le,i} = \sigma_{le,i} - \sigma_{le,i0} \quad (3.31)$$

Both  $\sigma_{le,i}$  and  $\sigma_{le,i0}$  in Equation (3.31) can be calculated by using Equation (3.15) if the element under consideration is situated at the crack initiator or by using Equation (3.18) if the element is situated at the crack tip. Index  $i0$  indicates the trough  $i0$  where the rain flow starts and flows over the peak  $i$  in the load history (see Figure 3.12 and the example given in Annex A.2.4) ;

2. Check if the newly calculated elastic-plastic stress  $\sigma_i$  or strain  $\varepsilon_i$  will be out of already ‘used’ stress-strain space, bounded by the stress and strain  $\sigma_{abs,i}$  and  $\varepsilon_{abs,i}$ . Check is made by using conditions given in Equations (3.32) or (3.33) :

$$|\sigma_i + \Delta\sigma_i| > \sigma_{abs,i} \quad (3.32)$$

$$|\varepsilon_i + \Delta\varepsilon_i| > \varepsilon_{abs,i} \quad (3.33)$$

3. If one of the conditions given in Equations (3.32) or (3.33) is true, then the calculation of the  $\sigma_i$  and  $\varepsilon_i$  is executed as indicated in step 3 of Figure 3.12. In this case the  $\sigma_i$  and  $\varepsilon_i$  will lay on the material cyclic stress-strain curve (Equation 3.19). The values of  $\sigma_{abs,i}$  and  $\varepsilon_{abs,i}$  will also change ;
4. If both of the conditions given in Equations (3.32) and (3.33) are false, then the calculation of the  $\sigma_i$  and  $\varepsilon_i$  is executed as indicated in step 4 of Figure 3.12.

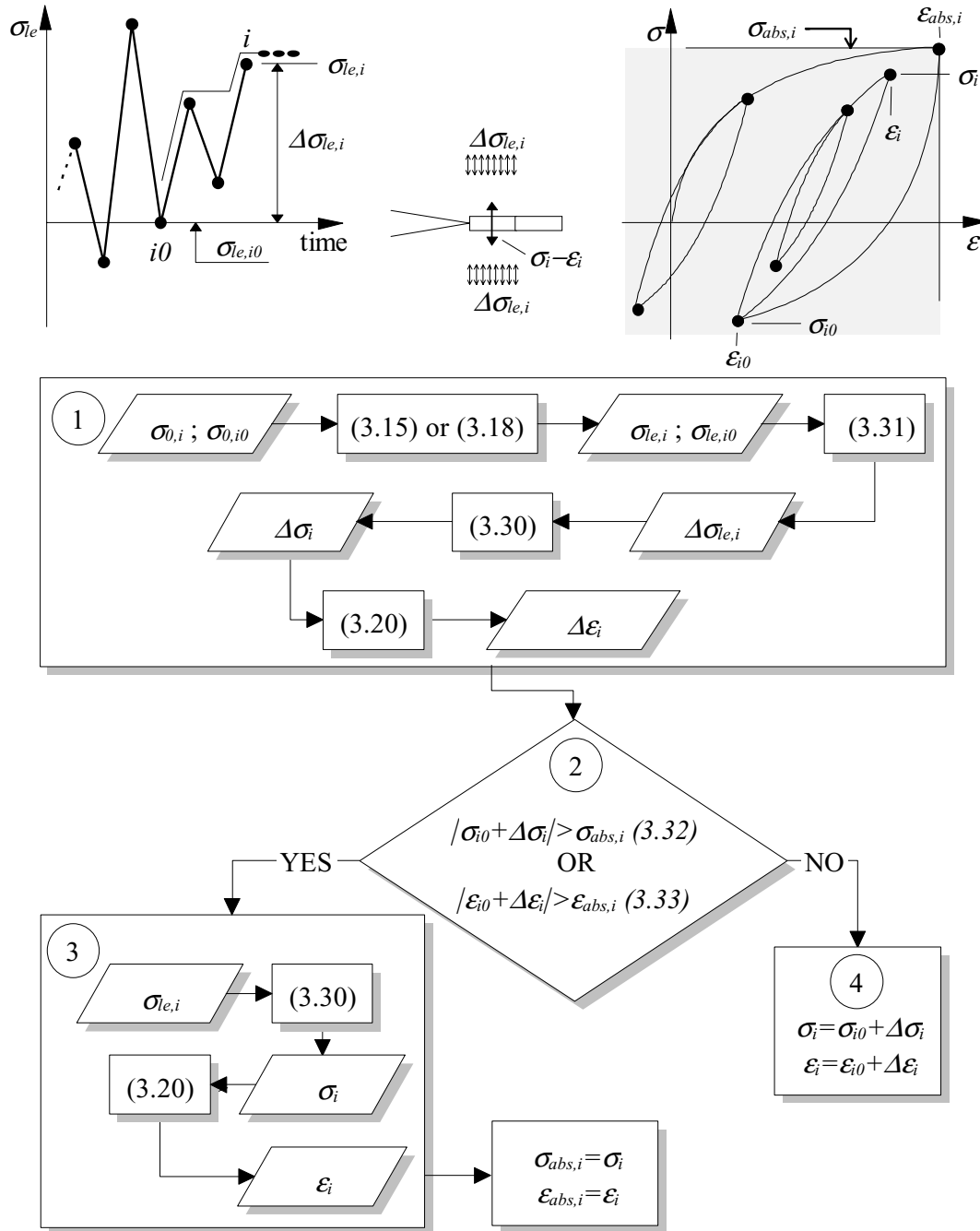


Figure 3.12 : Calculation algorithm of  $\sigma_i$  and  $\epsilon_i$ .

If the stress-strain hysteresis loops are calculated *correctly*, then they will stabilize after the occurrence of the first absolute maximum nominal stress peak. If the stress-strain hysteresis loops are calculated *incorrectly* (i.e. steps 2 and 3 are skipped), then the calculated hysteresis loops will not stabilize. Non-stabilized hysteresis loops result in incorrect local mean stress,  $\sigma_m$ , and consequently to an incorrect fatigue life of the element. The comparison of the correct and incorrect calculations of hysteresis loops is presented in Annex A.2.4.

Fabrication-introduced *residual stresses* also influence the position of the stress strain hysteresis loops. Their influence can be considered in the following manner. If the element under consideration is situated at the *crack initiator*, then the stress concentration factor,

$SCF(x)$ , used in Equation (3.15) must be calculated by using Equation (2.2). If the element under consideration is situated at the *crack tip*, then the stress intensity factor,  $K$ , used to evaluate the  $K_{eff}$  in Equation (3.18) must be calculated by using Equation (2.9) (also see Clause 3.3.3). An example of the influence of fabrication-induced residual stress on the position of stress-strain hysteresis loops is given in Annex A.2.4.

It can be concluded that the algorithm presented in Figure 3.12 allows the position of the stress-strain hysteresis loops of elements to be determined as a function of *any* loading history. The influence of *any* fabrication-induced *residual stress* is also considered.

### 3.4.2 Fatigue Life of the Element under Variable-Amplitude Loading

In this clause, the calculation of the fatigue life of the element in the case of variable-amplitude loading is presented. In order to determine the fatigue life of the element under variable-amplitude loading, the *linear damage accumulation concept* is used. The linear damage accumulation concept is usually used for constructional details (see Clause 2.3.4); however, herein it will be applied to the element.

In the previous clause, the calculation of the stress-strain *hysteresis loops* of the element as a function of variable-amplitude loading was given. Each hysteresis loop can be divided into two half-loops : the loading and the unloading half-loop. The elastic-plastic strain range  $\Delta\varepsilon_i$ , corresponding to the half-loop  $i$  can be calculated by using Equation (3.34) :

$$\Delta\varepsilon_i = \varepsilon_i - \varepsilon_{i^*} \tag{3.34}$$

where  $\varepsilon_i$  is the elastic-plastic strain at the tip  $i$  of the hysteresis loop. The tip  $i$  of the hysteresis loop corresponds to the load peak  $i$ . The  $\varepsilon_{i^*}$  is the elastic-plastic strain at the other tip of the same hysteresis loop. The elastic-plastic mean stress  $\sigma_{m,i}$ , corresponding to the half-loop  $i$  can be calculated by using Equation (3.35) :

$$\sigma_{m,i} = \frac{\sigma_i + \sigma_{i^*}}{2} \tag{3.35}$$

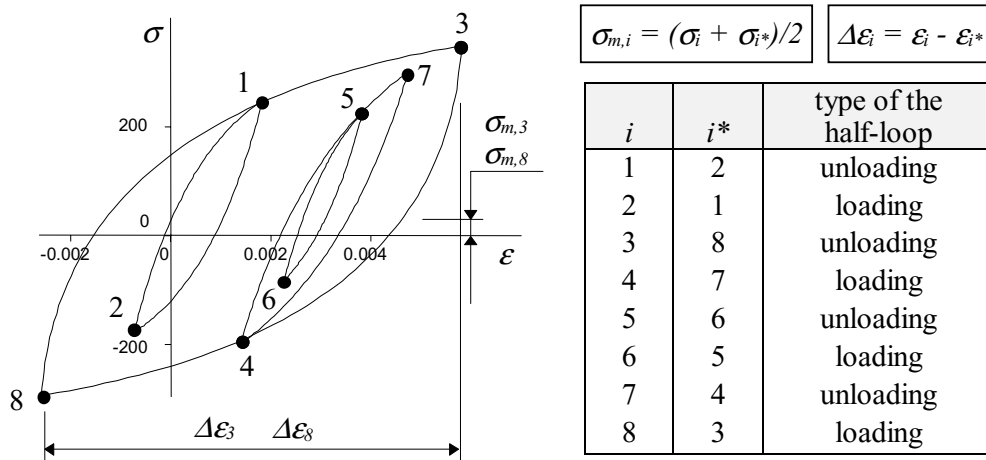


Figure 3.13 : Calculation of the elastic-plastic strain ranges and mean stresses.

where  $\sigma_i$  is the elastic-plastic stress at the tip  $i$  of the hysteresis loop and the  $\sigma_{i^*}$  is the elastic-plastic stress at the other tip of the same hysteresis loop. In Figure 3.13, four stress-strain hysteresis loops with the indexes of their tips are shown.

According to the linear damage accumulation rule, the damage due to the strain range  $\Delta\varepsilon_i$  and the mean stress  $\sigma_{m,i}$  is :

$$d_i = \frac{1}{2 \cdot N_{f,elem,i}} \quad (3.36)$$

where  $N_{f,elem,i}$  in Equation (3.36) can be calculated by using Equation (3.11) substituting the  $\Delta\varepsilon_i$  and  $\sigma_{m,i}$  for the  $\Delta\varepsilon$  and  $\sigma_m$  in Equation (3.11). Factor 2 in the same equation counts for the fact that damage is calculated for load reversal and not for load cycle. The fatigue life of the element can be calculated by tabulating damages  $d_i$  until the total damage of the element reaches 1 and by counting the number of terms in the sum. The algorithm of the determination of the fatigue life of the element under variable-amplitude loading consists of two steps (Figure 3.14) :

1. Increase of the element's damage  $D$  by the damage  $d_i$ .
2. Check if the element's total damage exceeds 1. If  $D \geq 1$ , then the element has failed at  $N_f$  cycles. Otherwise, step 1 is repeated with next load reversal  $i$ .

The algorithm presented in Figure 3.14 is valid for *any* load history.

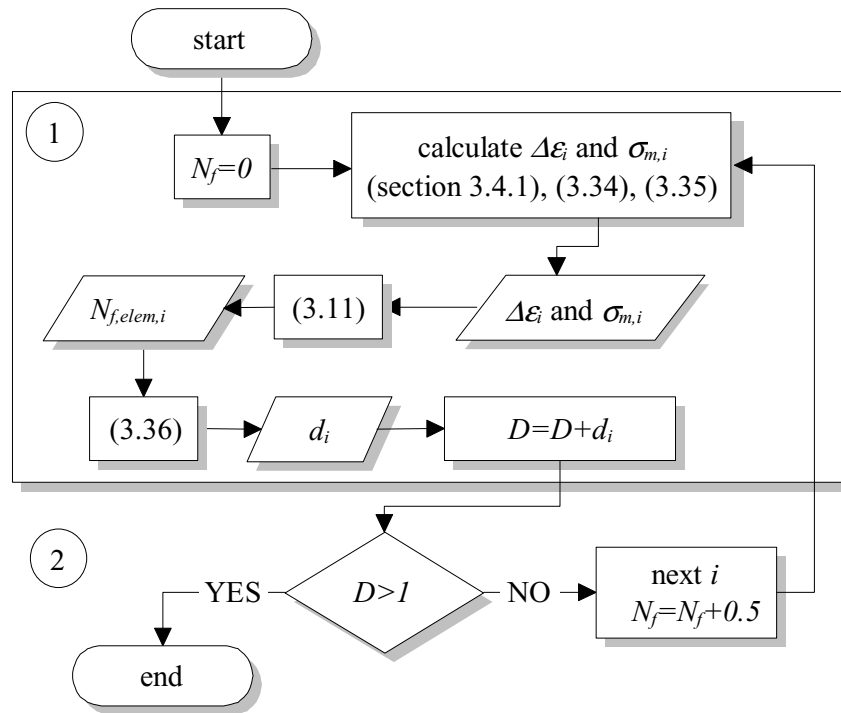


**Figure 3.14 :** Calculation algorithm of the fatigue life of the element under variable-amplitude loading.

It is interesting to note that the linear damage accumulation rule, if applied at the element scale, results in a damage accumulation curve that closely resembles the nonlinear damage accumulation curve of the detail (compare Figures 2.14 and 3.15).

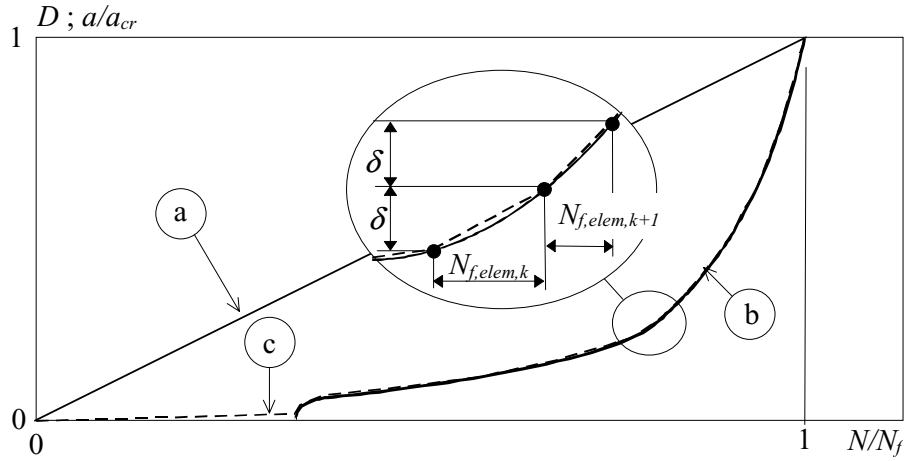


**Figure 3.15 :** Damage accumulation curves : a) linear curve, applied on detail's scale ; b) nonlinear curve ; c) linear curve, applied on element's scale.

### 3.4.3 Differentiation between Crack Initiation and Stable Crack Growth

In this clause a method which determines the crack propagation stage is introduced. It was shown in Clause 3.3.3 that the loading of the elements, depending upon their location, can be calculated in one of two ways: by using Equations (3.15) if the elements are situated at the crack initiator or by using Equation (3.18) if the elements are situated at the crack tip.

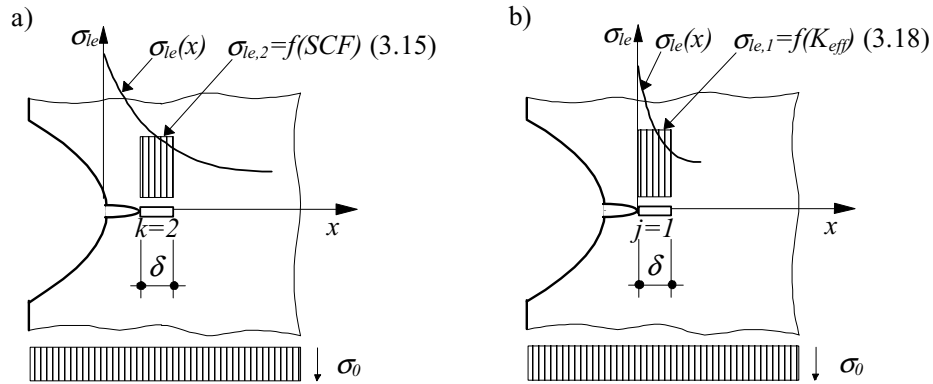


**Figure 3.16 :** Two possibilities to calculate loading of the element : a) using Equation (3.15) ; b) using Equation(3.18).

If a fatigue crack is very small ( $a=0.1$  to  $0.2$  mm), both Equations (3.15) and (3.18) can lead to almost the same loading of element,  $\sigma_{le}$ . (Figure 3.16). It is assumed that the change in the crack propagation stage occurs at the moment when both Equations (3.15) and (3.18) result in the same loading of the element. This is the criterion used to differentiate between the crack propagation stages: *crack initiation* occurs until condition (3.37) remains *true* ; if condition (3.37) becomes *false*, then the *stable crack growth* stage begins.

$$\sigma_{le}(SCF) > \sigma_{le}(K_{eff}) \tag{3.37}$$

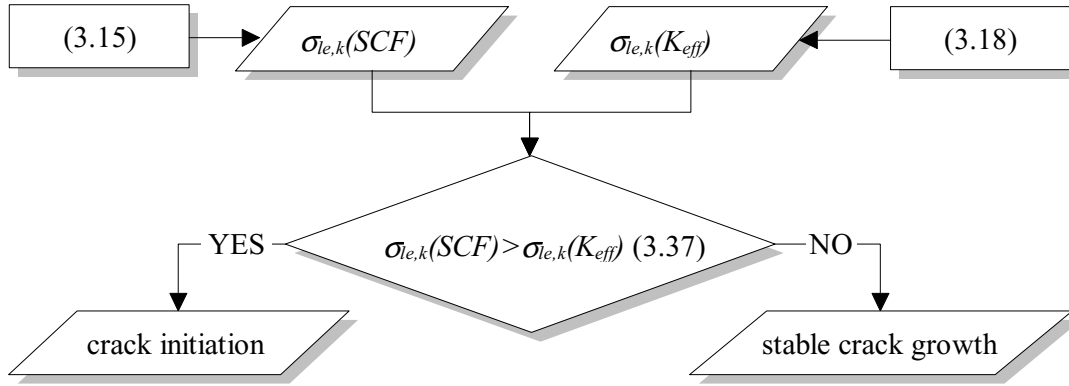


**Figure 3.17 :** Differentiation between the crack initiation and stable crack growth stages.

The differentiation between the crack propagation stages is explained in Figure 3.17: the crack initiation occurs until the loading of the element due to the linear-elastic stress field at the *crack initiator*,  $\sigma_{le}(SCF)$ , remains greater than the loading of the same element due to the linear-elastic stress field at the *crack tip*,  $\sigma_{le}(K_{eff})$ .

The method described above can be used if a detail is loaded with a constant-amplitude load. If *variable-amplitude* loads are applied to the detail, then condition (3.38) must be used instead of condition (3.37). The  $\Delta\sigma_{le}(SCF)$  and  $\Delta\sigma_{le}(\Delta K_{eff})$  in condition (3.38) must be calculated by using Equations (3.15) and (3.18) accordingly<sup>1</sup>.

$$\sum_{i=1}^{n_{rev}} \Delta\sigma_{le,i}(SCF) > \sum_{i=1}^{n_{rev}} \Delta\sigma_{le,i}(\Delta K_{eff}) \quad (3.38)$$

Annex A.2.5 presents a method to determine the initial crack length  $a_0$ . The calculations show that in most cases the initial crack length, depending on the geometry of the detail, is about 0.1 mm. This agrees with the data found in the literature [3.7], [3.8]. It can be concluded that in most cases, the crack initiation stage ends after the first element at the crack initiator fails. It is worth to mention that an experimental investigation is needed to verify and to justify a differentiation criterion established in this section.

### 3.4.4 Simultaneous Damaging of the Elements

The aim of this section is to introduce an important aspect that has to be considered in modeling: simultaneous damaging of the elements. All of the elements situated along the crack path are loaded simultaneously. This implies that all elements accumulate damage simultaneously. The loads applied to the elements close to the stress concentrator are high compared to the loads applied to the other elements. This means that the damage accumulation of the elements close to the stress concentrator occurs at a much faster rate than the damage accumulation of the other elements.

The simultaneous damaging of the elements depends upon the shape of the stress concentrators. For example, a notch creates more uniform stress field than a fatigue crack. This implies that the elements located at the notch are loaded more uniformly than the elements located at a fatigue crack (Figure 3.18). Consequently, the elements located at the notch are damaged more uniformly than the elements located at the fatigue crack. (In an extreme case, such as when the detail is without stress concentrators, the loads of all elements are equal and *all* elements should fail simultaneously).

<sup>1</sup> If the variable-amplitude load history contains a great amount of reversals, then the sum of the element loads can only be made by using the most damaging load reversals. This simplification can save computing time.

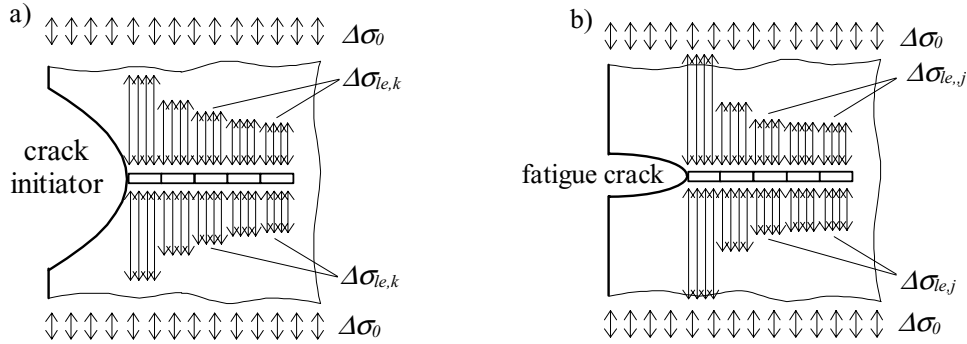


Figure 3.18 : Loading of the elements, situated : a) at crack initiator; b) at crack tip.

In order to optimize computing time, the number of the elements used in the calculations at the same time is taken  $n_{local} = 5$ . The influence of  $n_{local}$  on the results of simulation is shown in Clause 5.2.2.

At the failure of the element  $j=1$ , a new element is added to the crack path (Figure 3.19). This new element already has initial damage. It is assumed that a change in the damage gradient of the elements is constant which allows the initial damage of the new element to be estimated (Equation 3.39). It is interesting to note that in his notch stress-strain analysis approach to fatigue crack growth [3.6], Glinka accounts for the simultaneous damaging of the elements in the plastic zone. Glinka found that just after the failure of previous crack tip element, initial damage of the crack tip element is between 0.2 and 0.3.

$$D_{init,5} = \text{Max} \left( D_4 - \frac{(D_3 - D_4)^2}{D_2 - D_3}; 0 \right) \tag{3.39}$$

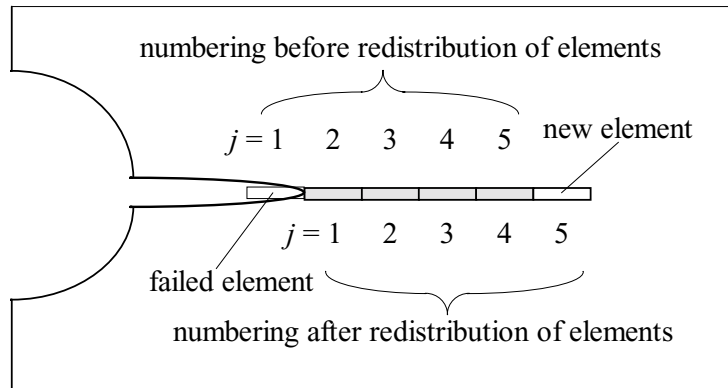


Figure 3.19 : Redistribution of the local elements after the failure of the first element.

It can be concluded that the importance of simultaneous damaging of elements on fatigue behavior is dependent upon the geometry of the stress concentrator. In order to save computing time, only 5 elements are used in the calculation at the same time. The algorithm to count for the simultaneous damaging of the elements is given in Figure 3.32.

### 3.5 CRACK CLOSURE MODEL

The crack closure phenomenon (Clause 2.3.3) is the main cause of acceleration or retardation in fatigue crack growth under variable-amplitude loading. This phenomenon must be accounted for when modeling variable-amplitude fatigue behavior. In this research, a new *crack closure model* has been developed in order to account for the effect of crack closure. The working principles and the calculation features of the crack closure model will be presented later.

### 3.5.1 Effective Stress Intensity Factor

The influence of the crack closure phenomenon on fatigue behavior can be modeled by using effective stress intensity concepts : effective stress intensity conception assumes that the cyclic stress field at the tip of a fatigue crack causes damage only when the crack is opened. Usually, a partial closure of the crack occurs even if nominal tensile loads are applied to the detail. This results in a *reduced* cyclic stress field at the crack tip. In order to account for the effect of a *reduced* cyclic stress field on the damaging of the crack tip, a reduced stress intensity factor, an *effective stress intensity factor*, must be introduced.

The effective stress intensity factor corresponding to load event  $i$ ,  $K_{eff,i}$ , can be calculated by using Equations (3.40) and (3.41) :

$$K_{eff,i} = K_i \quad \text{if} \quad K_i > K_{op} \quad (3.40)$$

$$K_{eff,i} = K_{op} \quad \text{if} \quad K_i < K_{op} \quad (3.41)$$

For all stress intensity factor peaks above the dotted line in Figure 3.20a, condition (3.40) must be regarded. For the stress intensity factor peaks below the dotted line in Figure 3.20a, condition (3.41) must be regarded. The *effective* stress intensity factor history is not the same as the stress intensity factor history (Figure 3.20b).

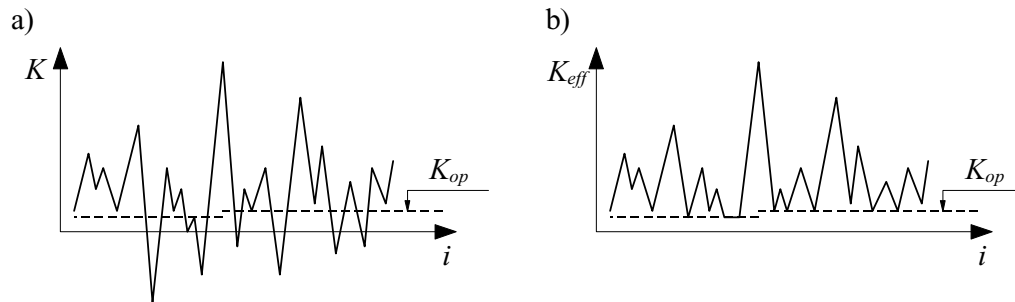


**Figure 3.20** : Stress intensity factor (SIF) histories : a) initial SIF history ; b) effective SIF history.

*Crack opening stress intensity factor*  $K_{op}$  in Equation (3.41) is a quantity which accounts for the non-linear dynamic behavior of the fatigue crack in elastically-plastically behaving solid.  $K_{op}$  depends on the nominal load history as well as the size of the crack, the shape of the plastic strip and the size of the plastic zone of the crack tip. The calculation of the crack opening stress intensity factor will be discussed in Clause 3.5.3.

### 3.5.2 Crack Opening Stress

If a detail is exposed to *constant-amplitude* loads, then the opening stress intensity factor  $K_{op}$  can be calculated by introducing crack opening stress  $\sigma_{op}$  in Equation (2.7). The *crack opening stress* is the *minimum* nominal stress which causes such an opening of the crack that there is no contact between crack edges. In this section, a simple method to calculate the crack opening stress  $\sigma_{op}$  is proposed.

Tests show that crack opening stress is a function of the ratio  $\sigma_{0,min}/\sigma_{0,max}$ , the stress state (plane stress or plane strain), and the ratio  $\sigma_{0,min}/\sigma'_{ys}$  [3.18], [3.19]. Under constant-amplitude load, the crack opening stress  $\sigma_{op}$ , attains a stable state after a relatively short stabilization period [3.20]. Plotting the crack opening stress  $\sigma_{op}$  versus the minimum nominal stress  $\sigma_{0,min}$  results in a bi-linear curve (Figure 3.21). The intersection point of both lines of the bi-linear curve occurs in the region where  $\sigma_{0,min} > 0$ . Tests show that the transition from one curve to another is smooth.

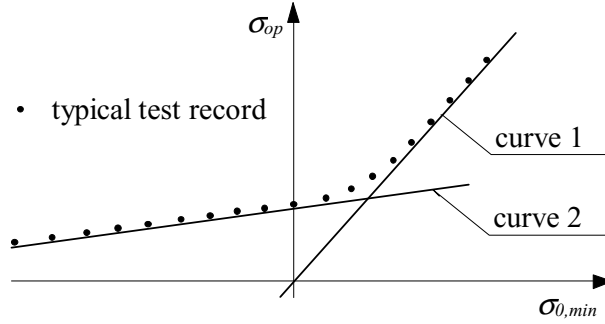


**Figure 3.21 :** A typical bi-linear plot of the crack opening stress versus the nominal minimum stress.

A large amount of the empirical formula for the  $\sigma_{op}$ , is available in the literature [3.7], [3.21], [3.22]. The disadvantage of these formulas is that they are only valid for limited values of  $\sigma_{0,min}$ ,  $\sigma_{0,max}$ , and  $pcf^1$ . A general crack opening stress formula does not exist. A study of the data of measured crack opening and existing crack opening stress equations revealed that the first curves given in Figure 3.21 can be determined by using Equation (3.42) :

$$\sigma_{op} = \sigma_{0,min} \quad (3.42)$$

and the second curve by using Equation (3.43) :

$$\sigma_{op} = \frac{\sigma_{0,max}}{1 + pcf} \cdot \left( 1 + \frac{\sigma_{0,min}}{\sigma'_{ys}} \right) \quad (3.43)$$

A general relationship for the crack opening stress  $\sigma_{op}$  is obtained by choosing the greater of the two values of  $\sigma_{op}$ . This leads to Equation (3.44) ( see Figure 3.22) :

$$\sigma_{op} = \text{Max} \left[ \sigma_{0,min}; \frac{\sigma_{0,max}}{1 + pcf} \cdot \left( 1 + \frac{\sigma_{0,min}}{\sigma'_{ys}} \right) \right] \quad (3.44)$$

<sup>1</sup> The plastic constraint factor  $pcf$  accounts for the plate thickness effect (Clause 2.3.3).

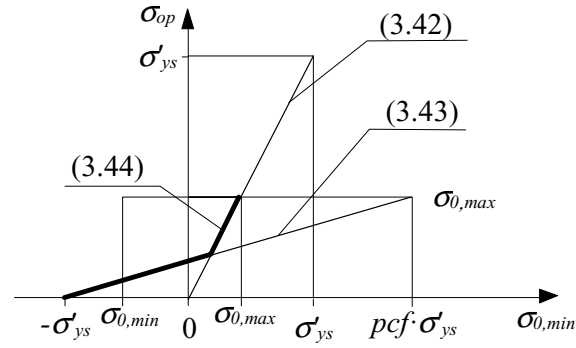


**Figure 3.22** : Graphical presentation of the relationship between  $\sigma_{op}$  and  $\sigma_{0,min}$ .

Crack opening stress changes as a function of the crack length; if a fatigue crack is very short then the crack opening stress  $\sigma_{op}$  almost equals the minimum nominal stress  $\sigma_{0,min}$ . Crack opening stress increases rapidly and attains its *stabilized* value  $\sigma_{op}$  at a crack length  $a=1$  to 2 mm. Crack opening stress as a function of the crack length can be calculated by using Equation (3.45), while the  $\sigma_{op}$  in Equation (3.45) must be calculated by using Equation (3.44), and  $\delta$  can be taken as 0.1 mm.

$$\sigma_{op}(a) = \sigma_{0,min} + \frac{Y(a-\delta)}{Y(a)} \cdot \frac{a-\delta}{a} \cdot (\sigma_{op} - \sigma_{0,min}) \quad (3.45)$$

Equation (3.45) is obtained through the study of the dynamic behavior of the Dugdale crack with plastic strip (see the following Clause). It was found that under constant-amplitude loading, the first contact point between Dugdale crack edges is obtained between the first plastic strip elements counted from the crack tip. It is assumed that the height of the plastic strip elements changes as a function of the stress intensity correction factor and crack length.

Equation (3.45) leads to a rapid stabilization of the crack opening stress  $\sigma_{op}(a)$  of the details of a high, but rapidly decreasing,  $Y$ -distribution. This type of  $Y$ -distribution is characteristic to welded details and Equation (3.45) leads to  $\sigma_{op}(a)$ -curves similar to those found in the literature [3.23]. On the other hand, if the  $Y$ -distribution is uniform, then both Equation (3.45) and the literature lead to a slower stabilization of the  $\sigma_{op}(a)$  [3.24]. It can be concluded that the crack opening stress  $\sigma_{op}$  stabilizes if the stress intensity correction factor  $Y$  has stabilized. The importance of Equation (3.45) is that it easily makes it possible to simulate a small crack behavior.

### 3.5.3 Crack Opening Stress Intensity Factor

The crack opening stress intensity factor is needed in order to calculate the effective stress intensity factor using Equations (3.40) and (3.41). The calculation of the crack opening stress intensity factor  $K_{op}$  for constant-amplitude loading can be made by using the crack opening stress  $\sigma_{op}$ . For a *variable-amplitude* loading however, the calculation of the crack opening stress intensity factor is more complicated than for a constant-amplitude loading. Complexity rises due to the need to account for the variable-amplitude load effects. In this section, it is explained how to calculate  $K_{op}$  for *any* variable-amplitude loading history.

Crack opening stress intensity factor  $K_{op}$  can be determined as a function of two parameters : the geometry of the crack *and* the nominal load history. The influence of the geometry of the crack is modeled by a *modified* Dugdale crack. The latter is modified by adding the *plastic*

strip along its edges<sup>1</sup> (Figure 3.23). The load history is taken into account by assuming that the  $K_{op}$  is influenced by the absolute maximum and minimum stress intensity factors, which are functions of the load history.

The following subjects will be reviewed further in this section; 1) considerations about the modeling of the plastic strip of the Dugdale crack are presented; 2) determination of the absolute maximum and absolute minimum stress intensity factors as function of the load history and the crack propagation, is shown ; 3) equations characterizing the Dugdale crack at the moment of its opening are derived ; and 4) the calculation of the crack opening stress intensity factor is given.

### **Dugdale Crack with Plastic Strip**

A real fatigue crack has a plastic strip at its edges. Therefore the plastic strip will also be added at the edges of Dugdale crack here. The plastic strip of the Dugdale crack edge is modeled using the plastic strip elements of width  $\delta$ . The width of the plastic strip elements is taken equal to the size of the crack tip elements. After the failure of the crack tip element, a new plastic strip element is added instead of a failed crack tip element. (Plastic strip elements are the broken crack tip elements (Figure 3.23)).

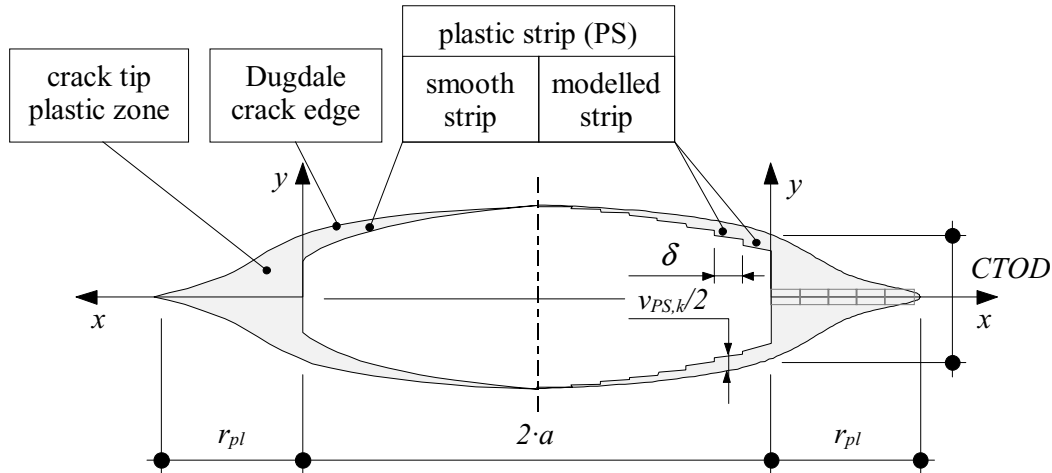


**Figure 3.23 : Dugdale crack with plastic strips at it's edges.**

There are two cases of evaluation of the height of the plastic strip elements :

1. it is assumed that the plastic strip remains unchanged unless the compressive nominal overload, equal to the cyclic yield stress,  $-\sigma'_{ys}$ , is applied on the detail. If the  $-\sigma'_{ys}$ , is applied on the detail, the height of *all* the plastic strip elements, is set to zero ;
2. if *crack tip* element fails, new *plastic strip* element is added at the location of the broken element (Figure 3.24). The height of the *new* plastic strip element,  $v_{PS,new}$ , is calculated using Equation (3.46).

$$v_{PS,new} = \frac{4}{\pi \cdot \sigma'_{ys} \cdot E} \cdot \left( \frac{K_{max,abs}^2}{pcf} - \frac{(K_{max,abs} - K_{op}^*)^2}{pcf + 1} \right) \quad (3.46)$$

<sup>1</sup> 'Classical' Dugdale crack does not have plastic strip along its edges, when a 'real' fatigue crack has plastic strip along its edges.

Equation (3.46) is developed substituting  $K_{max,abs}$  for the  $K$  in Equation (2.34) and  $(K_{max,abs} - K_{op}^*)$  for  $\Delta K$  in Equation (2.39); and subtracting of Equation (2.39) from Equation (2.34).  $K_{op}^*$  in Equation (3.46) can be calculated using Equation (3.47) :

$$K_{op}^* = \text{Max} \left[ K_{min,abs}; \frac{K_{max,abs}}{1 + pcf} \cdot \left( 1 + \frac{K_{min,abs}}{K(\sigma'_{ys})} \right) \right] \quad (3.47)$$

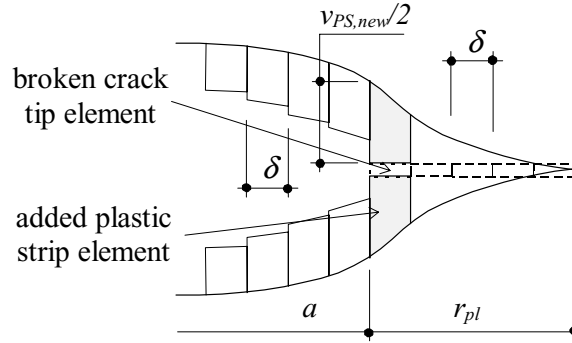


**Figure 3.24 :** New plastic strip element replaces failed crack tip element.

Equation (3.47) is similar to Equation (3.44) and is based on the assumption that under the constant-amplitude loading, the approach developed in this section should lead to the same opening stress intensity factor as the approach in section 3.5.2.  $K(\sigma'_{ys})$  in Equation (3.47) can be calculated using Equation (2.7), substituting the  $\sigma'_{ys}$  for the  $\sigma_0$  in Equation (2.7). Determination of the  $K_{max,abs}$  and the  $K_{min,abs}$  in Equation (3.47) is discussed later.

### ***Absolute Minimum and Maximum Stress Intensity Factors***

It is assumed that the influence of the load history on crack opening stress intensity factor,  $K_{op}$ , can be taken into account through two load history-related quantities : the absolute maximum and minimum stress intensity factors,  $K_{max,abs}$  and  $K_{min,abs}$ .

The influence of the  $K_{max,abs}$  on the crack behavior is kept in the ‘memory’ of the Dugdale crack by the size of its plastic zone,  $r_{pl}$ , where  $r_{pl}$  is a function of the stress intensity factor (Equation 2.33). It is assumed that due to irreversibility of the plastic deformations, the size of the plastic zone can change only in two cases :

1. the crack tip plastic zone size,  $r_{pl}$ , *increases* if the absolute maximum stress intensity factor,  $K_{max,abs}$ , increases. The size of the plastic zone due to  $K_{max,abs}$  can be calculated using Equation (3.48) :

$$r_{pl,max,abs} = \frac{\pi}{8} \cdot \left( \frac{K_{max,abs}}{pcf \cdot \sigma'_{ys}} \right)^2 \quad (3.48)$$

2. the crack tip plastic zone size,  $r_{pl}$ , *decreases* when crack advances. The size of the reduced plastic zone,  $r_{pl,max,pl}^*$ , can be calculated using Equation (3.49) (see Figure 3.25). Since the size of the plastic zone,  $r_{pl}$ , and the absolute maximum stress intensity factor,  $K_{max,abs}$ , are strictly related to each other, also the  $K_{max,abs}$  decreases if the  $r_{pl}$  decreases. The absolute maximum stress intensity factor just *after* crack advancement can be calculated using Equation (3.50), which is developed from Equation (3.48). Decreases of the absolute maximum stress intensity factor due to the decrease in the plastic zone during crack advancement is similar to the *reset stress* concept used by Veers [3.25] and Casciati and Colombi [3.26].

$$r_{pl,max,abs}^* = r_{pl,max,abs} - \delta \quad (3.49)$$

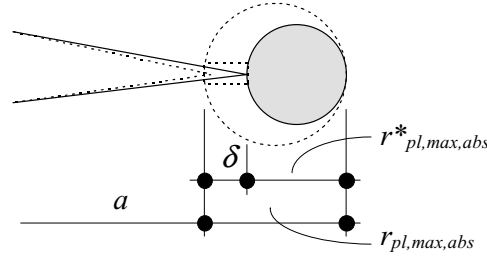


**Figure 3.25 :** Reduction of the crack tip plastic zone at the moment of the crack advance.

$$K_{max,abs} = psf \cdot \sigma'_{ys} \cdot \sqrt{\frac{\delta \cdot r_{pl,max,abs}^*}{\pi}} \quad (3.50)$$

The influence of the absolute *minimum* stress intensity factor,  $K_{min,abs}$ , is retained in the ‘memory’ of the Dugdale crack by the sizes of its *reverse* plastic zone,  $r'_{pl}$ . It is assumed that every time the size of the plastic zone,  $r_{pl}$ , changes, the influence of the previous load history is *erased* from the ‘memory’ of the crack and counting of the absolute minimum stress intensity factor must restart. Briefly, the absolute minimum stress intensity factor,  $K_{min,abs}$ , changes as a function of the absolute maximum stress intensity factor,  $K_{max,abs}$ . In the crack closure model, the  $K_{min,abs}$  is used in Equation (3.47), only.

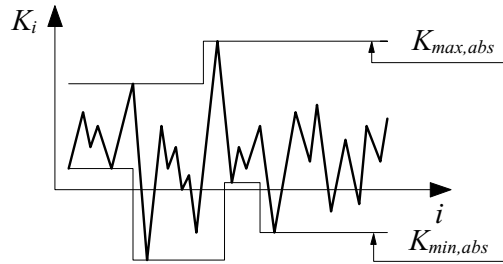


**Figure 3.26 :** Evolution of the  $K_{min,abs}$  as function of the  $K_{max,abs}$  and the load history.

Both  $K_{max,abs}$  and  $K_{min,abs}$  change as a function of the load history (Figure 3.26). The calculation algorithm of  $K_{max,abs}$ , and the  $K_{min,abs}$ , as a function of the load history is presented in Figure 3.27.

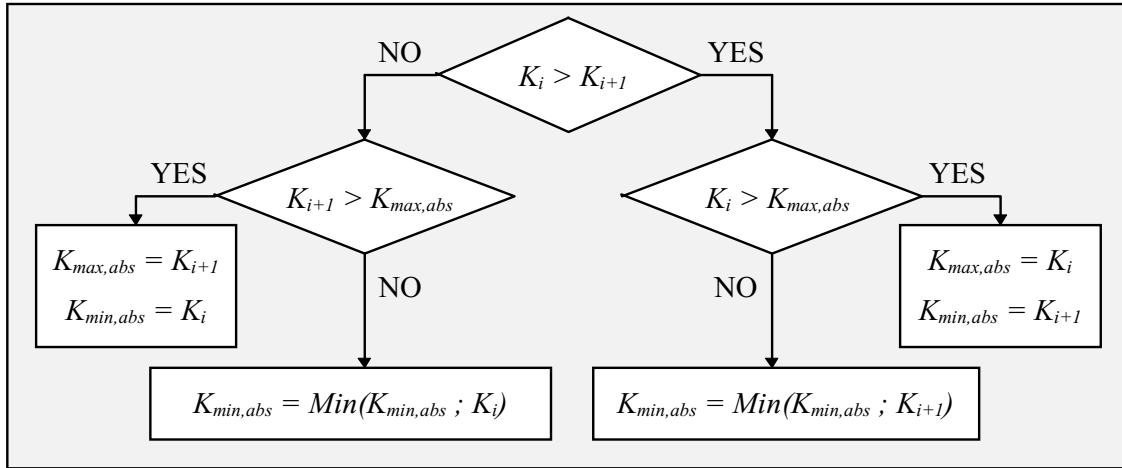


Figure 3.27 : Calculation algorithm of the  $K_{max,abs}$  and the  $K_{min,abs}$ .

### Dugdale Crack at Opening

It is possible to determine the opening stress intensity factor  $K_{op}$  from equations describing the dynamics of the Dugdale crack at the moment of its opening. These equations will be presented later. The moment the Dugdale crack becomes open is reached when no contact point exist between its edges. This moment can be expressed using two conditions :

- condition (3.51) states that at the moment the Dugdale crack is open, the crack opening displacement  $v_{op}(x_{cont})$  and the height of the plastic strip  $v_{PS}(x_{cont})$  at the *last* contact point of the crack edges  $x_{cont}$ , are equal :

$$v_{op}(x = x_{cont}) - v_{PS}(x = x_{cont}) = 0 \quad (3.51)$$

- condition (3.52) states that at the moment the Dugdale crack is open, all the other strip elements along  $x \in [0 \dots a]$ , must be *without* contact :

$$v_{op}(x \neq x_{cont}) - v_{PS}(x \neq x_{cont}) > 0 \quad (3.52)$$

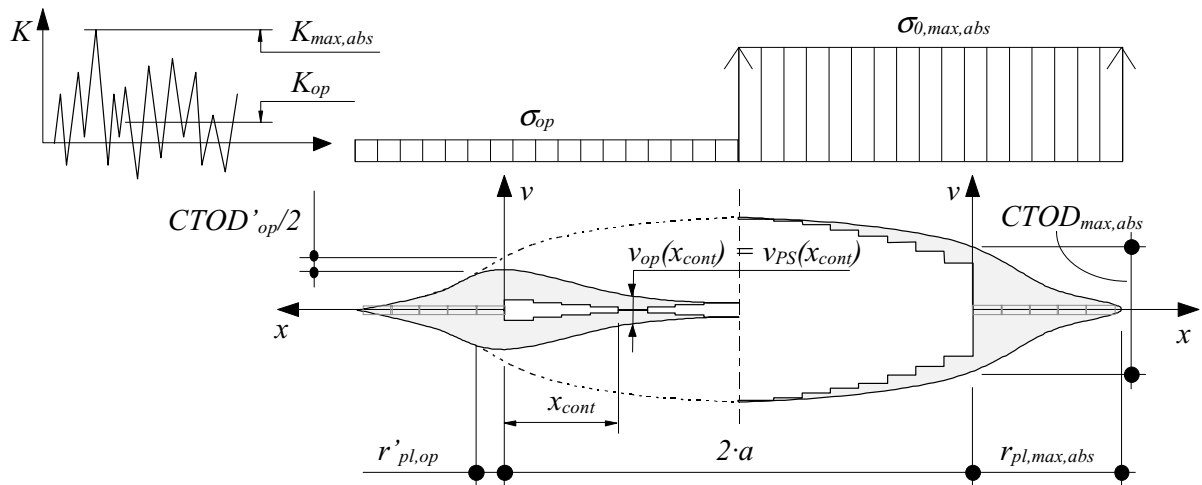


Figure 3.28 : Dugdale crack at the moment of its minimal (left side) and maximal (right side) opening.

The Dugdale crack at the moment it is open is shown on the left of Figure 3.28. The crack opening displacement at the last contact point  $x_{cont}$  at the moment of the crack is open,  $v_{op}(x_{cont})$ , can be expressed similarly to Equation (2.40), replacing the  $CTOD'$  in Equation (2.40) by the  $CTOD'_{op}$  :

$$v_{op}(x_{cont}) = v_{max,abs}(x_{cont}) - CTOD'_{op} \cdot g\left(\frac{x_{cont}}{r'_{pl,op}}\right) \quad (3.53)$$

The crack opening displacement at the last contact point  $x_{cont}$  due to the absolute maximum stress intensity factor,  $v_{abs,max}(x_{cont})$ , in Equation (3.53) can be calculated similarly to Equation (2.35) :

$$v_{max,abs}(x_{cont}) = CTOD_{max,abs} \cdot g\left(\frac{x_{cont}}{r'_{pl,max,abs}}\right) \quad (3.54)$$

The  $CTOD_{max,abs}$ , in Equations (3.53) and (3.54) is the crack opening displacement due to the  $K_{max,abs}$ , and can be calculated similar to Equation (2.34) :

$$CTOD_{max,abs} = \frac{4}{\pi} \cdot \frac{K_{max,abs}^2}{pcf \cdot \sigma'_{ys} \cdot E} \quad (3.55)$$

The size of the cyclic plastic zone at the moment of the crack is open,  $r'_{pl,op}$ , in Equation (3.53), can be calculated similarly to Equation (2.37), by replacing the  $\Delta K$  in Equation (2.37) by the  $(K_{max,abs} - K_{op})$  :

$$r'_{op} = \frac{\pi}{8} \cdot \left(\frac{K_{max,abs} - K_{op}}{(pcf + 1) \cdot \sigma'_{ys}}\right)^2 \quad (3.56)$$

The cyclic crack opening displacement at the moment the crack is open,  $CTOD'_{op}$  in Equation (3.53) can be calculated similar to Equation (2.39), by substituting  $(K_{max,abs} - K_{op})$  for the  $\Delta K$  in Equation (2.39) :

$$CTOD'_{op} = \frac{4}{\pi} \cdot \frac{(K_{max,abs} - K_{op})^2}{(pcf + 1) \cdot \sigma'_{ys} \cdot E} \quad (3.57)$$

### **Crack Opening Stress Intensity Factor**

The crack opening stress intensity factor  $K_{op}$  must be determined by an *iteration* process of equations (3.51) and (3.52). The values  $v_{PS}$  and  $x_{cont}$  in equations (3.51) and (3.52) are taken from the array of the plastic strip elements. The crack opening displacement  $v_{op}$  in conditions (3.51) and (3.52) can be calculated according to the algorithm, presented in Figure 3.29, where  $K_{max,abs}$  can be determined according to the algorithm in Figure 3.27.  $K_{op}$  and  $x_{cont}$  in iteration process must be varied until conditions (3.51) and (3.52) become true. It can be added that the  $K_{op}$  must be redefined each time the  $K_{max,abs}$  changes.

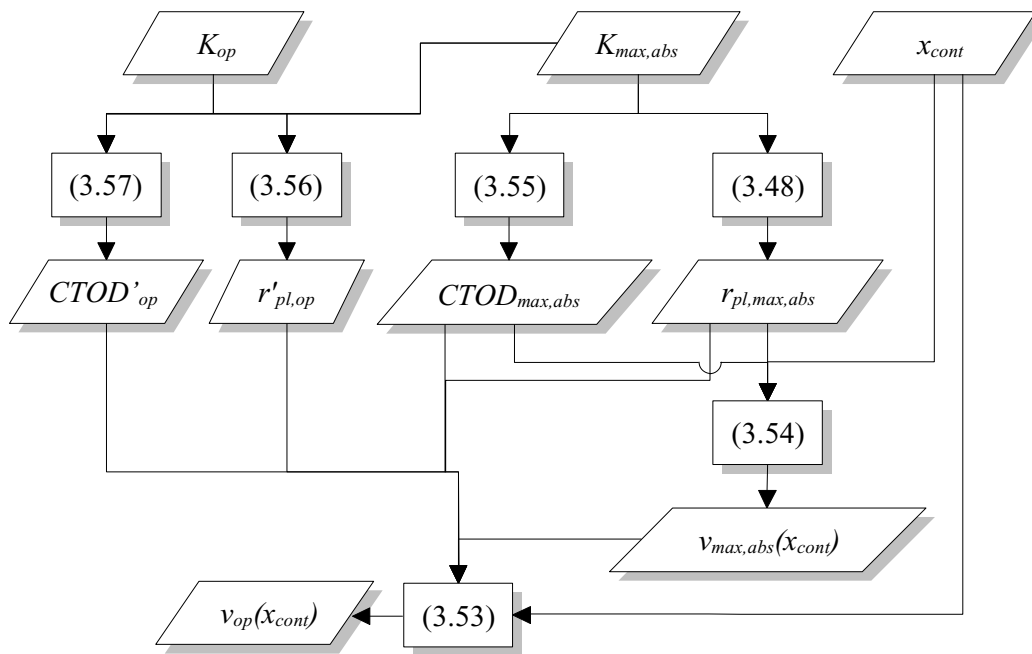


**Figure 3.29 :** Calculation algorithm of the Dugdale crack opening displacement at the unique contact point between crack edges.

It can be concluded that crack closure model developed can determine the effective stress intensity factor as a function of *any* load history. The crack closure model is verified in Chapter 4.

### 3.6 MODEL ALGORITHM

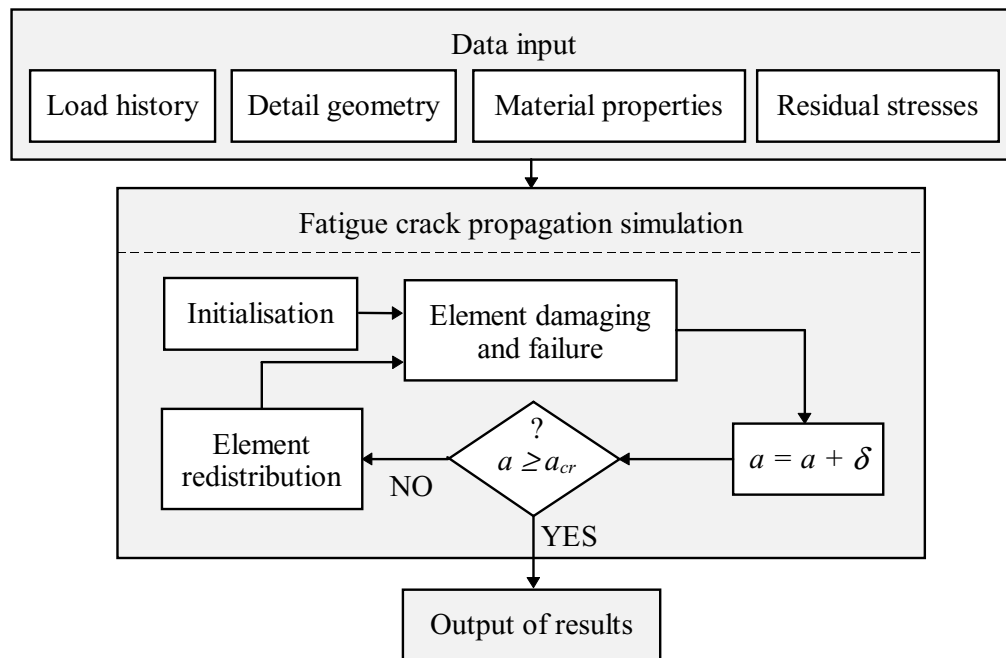


**Figure 3.30 :** The overall algorithm of the 'model F'.

On the basis of the principles and details for modeling presented in chapter 3, a computer program has been developed, called ‘model F’ where F stands for ‘fatigue’. C++ was chosen as the programming language due to its power and the ability to use the object-oriented approach, [3.27]. The aim of this section is to present the working algorithm of the ‘model F’. The overall algorithm of the ‘model F’ is shown in Figure 3.30. It contains three main steps : the data input, fatigue crack propagation simulation, and the output of results. These steps are briefly explained in this section.

### 3.6.1 Data Input

As shown in Figure 3.30, three groups of input data must be given : the load history, the geometry of the detail and the material properties. Input is made using data files.

#### *Load History*

The load history is introduced into the model as series of constant-amplitude load blocks, where each block contains three components : number of load cycles in the block,  $n$ , minimum load of the block,  $\sigma_{0,min}$ , and maximum load of the block,  $\sigma_{0,max}$ . To introduce the variable-amplitude load history,  $n$  is taken as 1. The rainflow analysis of the load history, needed to calculate the stress-strain hysteresis loops of elements, is integrated into the program.

#### *Geometry of Detail*

The geometry of the detail is normalized using two parameters : the stress concentration factor distribution,  $SCF(x)$ , and the stress intensity correction factor distribution,  $Y(a)$ , where the  $x$  and  $a$  are the coordinates along crack path. The plastic constraint factor,  $pcf$ , is also part of the geometrical data as it takes into account plate thickness effect. The ‘model F’ has a built-in library where the most often solutions of  $SCF(x)$  and  $Y(a)$  are given.

#### *Material Properties*

For the calculation, eight material constants must be known : the cyclic yield stress  $\sigma'_{ys}$ , elastic modulus,  $E$ , two constants of the Ramberg-Osgood equations ( $K'$ ,  $n'$ ), and four constants of the strain-life relationship ( $\sigma'_f$ ,  $b'$ ,  $\epsilon'_f$ ,  $c'$ ). These material data can be simply obtained for example from [3.9].

#### *Residual Stresses*

Fabrication-introduced residual stresses are introduced as a table of two columns where the first column corresponds to the coordinate  $x$  situating along the crack propagation path, and the second column to the residual stress at coordinate  $x$ ,  $\sigma_{res}(x)$ .

### 3.6.2 Fatigue Crack Propagation Simulation

In this section the algorithm of the main part of the ‘model F’ - crack propagation simulation module is explained. First the program is initialized. Then the fatigue crack propagation calculation is carried out. Calculation of the fatigue crack propagation consists of continuous damaging and failure of elements until the critical crack length  $a_{cr}$  is reached (Figure 3.30). A critical crack length  $a_{cr}$  is considered as an input parameter of the model. Its value can be determined from the resistance criterion of the net section of the detail, or using fracture toughness of the material,  $K_{IC}$  [3.28].

#### *Initialization*

The initialization consists of two tasks. First, the element mesh is generated with the elements placed close to the stress concentrators (Figure 3.1). No more than 5 elements should be used at the same time in the calculations. Second, the variables are initialized : input data is

assigned to the variables and the arguments of the objects. The use of objects in programming makes it possible to create very complex relations between the different parts of the model without losing control over the function of the program. It also provides flexibility for further developments of the model [3.29], [3.30].

### Element Damaging and Failure

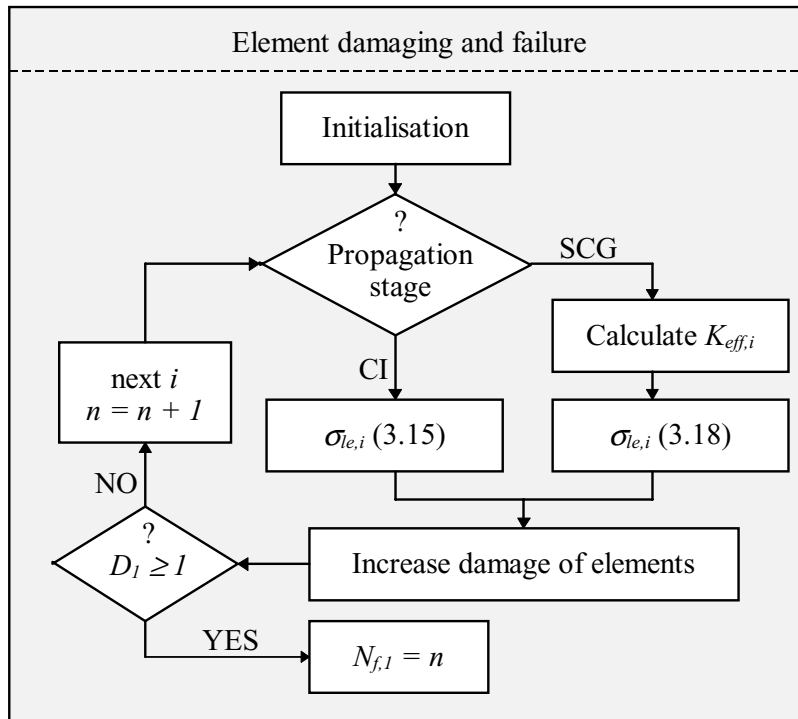


Figure 3.31 : Detail of the algorithm in Figure 3.30 : element damaging and failure.

The algorithm for the calculation of failure and the simultaneous damaging of the elements is presented in Figure 3.31. It contains the following steps :

*Initialization* of the damage calculation loop consists of; 1) the initialization of the counter of load reversals,  $n$ , and; 2) the calculation of the crack propagation stage which can be made as indicated in Clause 3.4.3. Determination of the crack propagation stage is needed if the crack initiation has not yet changed into a stable crack growth. Later, when stable crack growth prevails, this step can be skipped.

*Switch* to valid crack propagation stage : if the stable crack growth stage prevails, then the calculation of the effective stress intensity factor  $K_{eff,i}$ , for current the load event,  $i$ , is needed.  $K_{eff,i}$  can be determined using the crack closure model described in Section 3.5. Depending on the crack propagation stage, Equations (3.15) or (3.18) must be used to calculate the *linear elastic stress*  $\sigma_{le,i}$ , for each element  $j$ .

*Increase in damage of elements* can be made according to Figure 3.32. The damage increment due to load reversal  $i$ ,  $d_i$ , is added to *all* five elements, and depends on the element load  $\sigma_{le,i}$ . Calculation of  $d_i$  as function of the element load  $\sigma_{le,i}$  can be made using the principles given in Clauses 3.35, 3.41, 3.42.

After the damage increment, it is *checked* if the failure criterion of the first element,  $D_1 = 1$ , is satisfied. If the first element has failed, then the count of the load reversals indicates the

fatigue life of the failed element :  $N_{f,i} = n$ . If not, the count of load reversals  $n$  is increase by 1 and the calculation loop is repeated with the next load reversal  $i$ .

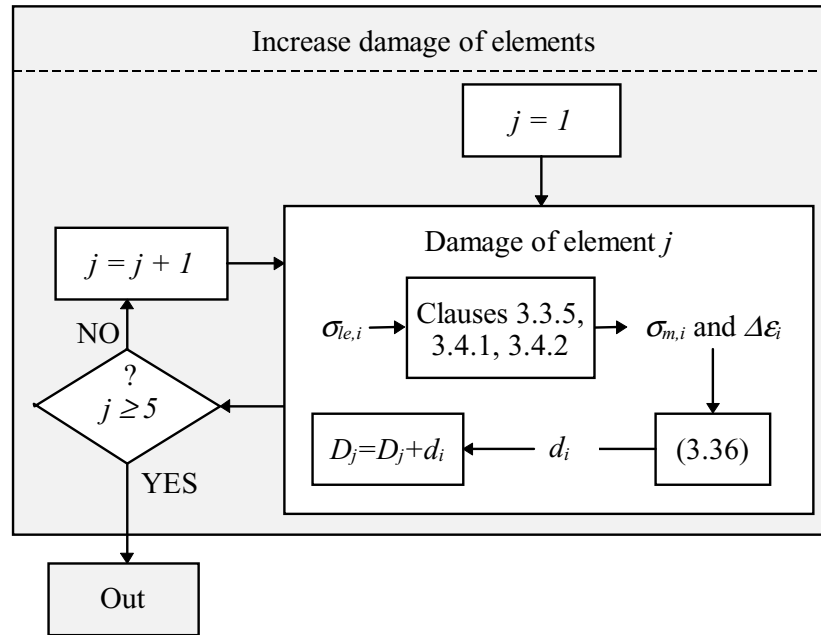


Figure 3.32 : Detail of the algorithm in Figure 3.31 : increase damage of elements.

### Crack Advance and Element Redistribution

After the failure of the element closest to the stress concentrator, the crack length  $a$  is increased by the element size  $\delta$ . It is then verified if crack length  $a$  exceeds the critical crack length  $a_{cr}$ . If the crack does not exceed the critical size, the elements are redistributed, otherwise, the output is written.

Element redistribution consists of decreasing the local counting of elements by,  $j=j-1$  : the second element becomes the first, the third element becomes the second etc.. The element that has failed is removed and a new element is added next to the last local element (Figure 3.19). If the position of the new element is above the critical crack length, then a new element is not added to the set of the elements. The initial damage of added element is calculated using Equation (3.39).

### 3.6.3 Output of Results

The primary result from the analysis is the fatigue life of the detail  $N_f$ . However, many other variables have to be calculated in order to reach  $N_f$ . During the calculation, these variables are kept and can help to analyze the simulated crack propagation in details. These variables are called *additional* results and are saved after each crack advances, before redistribution of elements. The additional results, given as functions of the crack length are :

- the number of load cycles  $N(a)$  ;
- the mean crack propagation rate within an element,  $da/dN(a)$ , which can be calculated by dividing element size by its fatigue life ;
- the equivalent constant-amplitude stress intensity factor range  $\Delta K_{eq}(a)$ . This parameter is introduced in order to normalize the influence of variable-amplitude loading.  $\Delta K_{eq}$  can be

calculated using the algorithm given in Figure 3.33, where  $\Delta K_{eq}$  is a function of  $\Delta\sigma_{le}$  in Figure 3.33 and can be calculated using Equation (3.58)<sup>1</sup>.

$$\Delta K_{eq} = \Delta\sigma_{le} \cdot \sqrt{\frac{\pi \cdot \delta}{2}} \quad (3.58)$$

- opening stress intensity factor  $K_{op}(a)$  ;
- height of the new plastic strip element, added failed crack tip element's place,  $v_{PS,new}(a)$  ;
- change in the crack propagation stage : transformation of the crack initiation into stable crack growth stage.

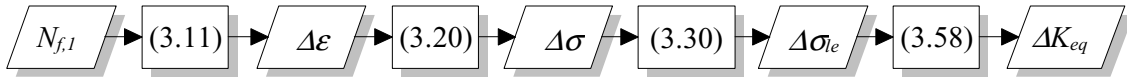


Figure 3.33 : The calculation algorithm of  $\Delta K_{eq}$ .

## 3.7 SUMMARY AND CONCLUSIONS

### *Representation of Crack Propagation Path*

The fatigue crack propagation path is represented by uni-dimensional elements. The first element is situated at the stress concentrator and the other elements are placed side by side along the crack propagation path. It is assumed that each element represents the average material behavior of a local region around it. In order to differentiate between the elements, they are numbered according to two systems : local numbering and global numbering.

The minimum and maximum size of elements is determined by the following requirements : elements must be many times greater than material grain size and should be smaller than the minimum possible size of the plastic zone around the stress concentrator. These two requirements lead to the average element size for steel :  $\delta = 0.1 \pm 0.05$  mm.

### *Fatigue of Elements*

The fatigue life of the detail can be calculated as the sum of the fatigue lives of the elements. In order to calculate the fatigue life of the elements, a convenient load-life relationship must be chosen. Due to its advantages compared to other load-life relationships, the strain-life relationship is selected to calculate fatigue life of elements.

Use of the strain-life relationship implies that that fatigue life of element is function of the elastic-plastic strain range and mean stress. Both quantities can be determined from the elastic-plastic stress-strain hysteresis loops of element. The hysteresis loops of the element result from the cyclic loading of the elements. It is assumed that each element is loaded by the linear-elastic cyclic stress range which is a function of the linear-elastic cyclic stress field around the stress concentrator. Glinka's equivalent strain energy density criterion is used to calculate the elastic-plastic stress-strain hysteresis loops as a function of a linear-elastic loading of elements.

### *Selected Aspects of Modeling*

There are some aspects of modeling that have to be explained : a variable-amplitude loading history evokes additional features implied in the calculation of the stress-strain hysteresis loops of the elements ; the linear damage accumulation concept is applied in order to calculate

<sup>1</sup> Equation (3.58) is got from Equation (3.18), taking  $j = 1$ , substituting  $\sigma_{le,j}$  and  $K_i$  for the  $\Delta\sigma_{le}$  and  $\Delta K_{eq}$  in Equation (3.18), and solving Equation (3.18) for the  $\Delta K_{eq}$ .

the element fatigue life under variable-amplitude loading ; all the elements accumulate fatigue damage simultaneously is taken into account in the modeling.

In addition, it appears that the developed approach makes permits differentiation between the crack initiation and the stable crack growth stages : the loading of elements can be calculated using two methods, the first method, based on the stress concentration factor, corresponds to the crack initiation stage. The second method, based on the stress intensity factor, corresponds to the stable crack growth stage. The crack initiation changes into the stable crack growth at the moment both methods result in the same element load.

### ***Crack Closure Model***

In order to take into account the variable-amplitude load effects, the *effective* stress intensity factor must be used in calculations instead of the stress intensity factor. The former depends on the *opening* stress intensity factor. In order to calculate the opening stress intensity factor, an original crack closure model is created.

The crack closure model is based on the dynamic analysis of a modified Dugdale crack : the Dugdale crack is modified by adding the plastic strip elements at the edges. The equations of the Dugdale crack opening displacement at the instant of crack opening allow iteration of the opening stress intensity factor. In addition, two simple equation are developed in order to calculate the crack opening stress in the case of the constant-amplitude loading.

### ***Modeling Algorithm***

A computer program called ‘model F’ is developed on the basis of the established modeling principles, and the algorithm given. The algorithm has three steps : input of the data, simulation of the fatigue crack propagation, and output of the results. The input contains four groups of data : the load history, the geometry of the detail, the material properties, and the residual stresses. The fatigue crack propagation simulation consists in continuous calculation of the damage accumulation and failure of elements. After each failure of elements, the crack length increases by element size. Calculations are continued until the fatigue crack reaches its critical size. The output contains the fatigue life of the detail, as well as a set of the crack propagation related data which help the analysis of simulation results.

